รายงานวิจัยฉบับสมบูรณ์

โครงการ การวิเคราะห์เชิงอณูชีวฟิสิกส์ของการเกิดรูรั่วในผนังเนื้อเยื่อสังเคราะห์ที่เกิดขึ้นโดยชิ้นส่วนโปรตีนสารพิษจาก *Bacillus thuringiensis*

Molecular Biophysical Analysis of Pore-Formation in Artificial Membranes by a Putative Transmembrane Fragment of a *Bacillus thuringiensis* δ-Endotoxin

โดย นายชนันท์ อังศุธนสมบัติ

30 พฤศจิกายน 2543

สัญญาเลขที่ RSA/12/2540

รายงานวิจัยฉบับสมบูรณ์

โครงการ การวิเคราะห์เชิงอณูชีวฟิสิกส์ของการเกิดรูรั่วในผนังเนื้อเยื่อสังเคราะห์ที่เกิดขึ้นโดยชิ้นส่วนโปรตีนสารพิษจาก *Bacillus thuringiensis*

Molecular Biophysical Analysis of Pore-Formation in Artificial Membranes by a Putative Transmembrane Fragment of a *Bacillus thuringiensis* δ-Endotoxin

ผู้วิจัย
นายชนันท์ อังศุธนสมบัติ

สังกัด
สถาบันอณูชีววิทยาและพันธุศาสตร์
มหาวิทยาลัยมหิดล

สนับสนุนโดยสำนักงานกองทุนสนับสนุนการวิจัย

Acknowledgements

I am grateful to Prof. Sakol Panyim and Prof. Propon Wilairat for valuable comments, to Drs G. Katzenmeier, C. Krittanai and A. Ketterman for helpful discussion and to P. Uawithya, J. Kittiworakan, S. Leetacheewa, U. Chanama and A. Nirachanon for technical assistance. Cry4B antibodies were kindly provided by Prof. David Ellar, University of Cambridge, England. This work was supported in part by the Thailand Research Fund. Golden Jubilee Ph.D. research scholarships to Issra Sramala and Theeraporn Puntheeranurak are gratefully acknowledged.

Chanan Angsuthanasombat

November 30, 2000

Project Code : RSA40-8-0012

Project Title :

Molecular Biophysical Analysis of Pore-Formation in Artificial Membranes by a Putative Transmembrane Fragment of a *Bacillus thuringiensis* δ-Endotoxin

การวิเคราะห์เชิงอณูชีวฟิสิกส์ของการเกิดรูรั่วในผนังเนื้อเยื่อสังเคราะห์ที่เกิดขึ้นโดยชิ้นส่วนโปรตีนสารพิษจาก *Bacillus thuringiensis*

Investigator : Chanan Angsuthanasombat, Ph.D.
Institute of Molecular Biology and Genetics,
Mahidol University

E-mail Address : stcas@mahidol.ac.th

Project Period : 3 years (December 1, 1997 - November 30, 2000)

Abstract

The different Cry δ-endotoxins produced by *Bacillus thuringiensis* have been shown to kill susceptible insect larvae by forming a lytic pore in the target midgut epithelial cell membrane. In the previous studies, we have shown that tryptic activation of the 130-kDa Cry4B toxin produced protease-resistant products of ca. 47 kDa and ca. 21 kDa. The 21-kDa fragment was identified to be the N-terminal five-helix bundle (α1-α5) which is a potential candidate for membrane insertion and pore formation.

In this report, we have constructed the recombinant clone over-expressing the putative pore-forming (PPF) fragment (α1-α5) as inclusion bodies in *Escherichia coli*. The partially purified inclusions were composed of a 23-kDa protein which cross-reacted with Cry4B antibodies and whose N-terminus was identical to that of the 130-kDa protein. Dissimilar to protoxin inclusions, the PPF inclusions were only soluble when the carbonate buffer, pH 9.0 was supplemented with 6 M urea. After renaturation *via* stepwise dialysis, the refolded PPF protein appeared to exist as an oligomer and was structurally stable upon trypsin treatment. Unlike the 130-kDa protoxin, the refolded protein was able to release entrapped glucose from liposomes comparable to the activated toxin, although it lacks larvicidal activity against *Aedes aegypti*.. These results therefore support the notion that the PPF fragment consisting of α1-α5 of the activated Cry4B toxin is involved in membrane pore-formation.

We have also employed single proline substitutions *via* PCR-based mutagenesis and demonstrated that helices 4 and 5 in the pore-forming domain of the Cry4B toxin are essential for mosquito-larvicidal activity, likely to be involved in pore formation rather than in receptor binding. To further identify critical residues for toxicity, substitutions with alanine of each of the charged amino acids (Arg-143, Lys-156, Arg-158 and Glu-159) and one polar residues (Asn-151) in the transmembrane helix 4 were performed. Similar to the wild-type Cry4B protoxin, all five mutant toxins were over-expressed as cytoplasmic inclusions in *E. coli* and were structurally stable upon solubilisation and trypsin activation in carbonate buffer, pH 9.0. Interestingly, a complete loss of activity against *A. aegypti* larvae was observed for the alanine substitution at Arg-158, while replacements at the four other positions did not affect the toxicity. The results reveal a crucial role in toxin function for the positively charged side chain of Arg-158 in helix 4 of the Cry4B toxin.

The putative transmembrane segments, helices 4 and 5 were further studied by means of nanosecond molecular dynamics (MD) simulation. The α4-α5 hairpin (residues Gln140-Glu198) was truncated from a 3D homology model of Cry4B and inserted into a fully hydrated lipid bilayer. It adopts a stable helical hairpin-liked structure of which the amphipathic α4 was stabilised by favorable interactions between pockets of membrane-penetrating water molecules and side chains of polar residues while the relatively hydrophobic α5 appeared to unwind at its C-terminus. Unrestrained MD simulations were performed with a model pore consisting of six copies of the α4-α5 hairpin in a fully hydrated lipid bilayer with Arg-158 pointing inward to pore lumen. Predicted conductance values suggested that the transmembrane α4-α5 hairpin of Cry4B has a potential to form a stable oligemeric pore with 2-3 nm in diameter.

บทคัดย่อ

กลไกการออกฤทธิ์ของโปรตีนสารพิษแต่ละชนิดจากแบคทีเรีย *Bacillus thuringiensis* (Bt) นั้นเชื่อว่าเกี่ยวข้องกับการเกิดรูรั่วที่ผนังเนื้อเยื่อเซลล์บุผิวกระเพาะอาหารส่วนกลางในตัวหนอนแมลงที่กินโปรตีนสารพิษนี้เข้าไป จากการศึกษาเบื้องต้นพบว่า โปรตีนสารพิษชนิด Cry4B ขนาด 130 กิโลดาลตัน ซึ่งเมื่อถูกกระตุ้นด้วยเอนไซม์ trypsin จะได้ชิ้นส่วนโปรตีนขนาดประมาณ 47 และ 21 กิโลดาลตัน โดยที่ชิ้น 21 กิโลดาลตัน มีองค์ประกอบเป็นเกลียวอัลฟาที่ 1-5 ซึ่งเชื่อว่าจะเป็นส่วนที่สอดแทรกเข้าไปในผนังเนื้อเยื่อทำให้เกิดรูรั่ว โครงการนี้มีวัตถุประสงค์เพื่อการศึกษาหาข้อมูลพื้นฐานที่จะนำไปสู่ความเข้าใจมากยิ่งขึ้นเกี่ยวกับกลไกการสอดแทรกและการทำให้เกิดรูรั่วในผนังเนื้อเยื่อที่เกิดโดยโปรตีนสารพิษชนิด Cry4B

ในรายงานนี้ เราได้ใช้เชื้อ *E. coli* ในการสร้างชิ้นส่วนโปรตีน PPF ซึ่งเป็นส่วนเกลียวอัลฟาที่ 1-5 ดังกล่าวเป็นปริมาณมาก และอยู่ในรูปของผลึกโปรตีนที่ไม่ละลาย ซึ่งเมื่อนำมาแยกบริสุทธิ์เบื้องต้น

พบว่า ผลึกโปรตีนดังกล่าวประกอบด้วยโปรตีนขนาด 23 กิโลดาลตัน และสามารถจับตัวกับ Cry4B antibodies ได้อย่างจำเพาะเจาะจง และยังพบว่า ลำดับกรดอะมิโนทางด้านปลายอะมิโนเหมือนกับของโปรตีนสารพิษ Cry4B ขนาด 130 กิโลดาลตัน อย่างไรก็ตามผลึกโปรตีน PPF นี้จะสามารถละลายได้ในตัวทำละลายที่มี 6M urea โปรตีน PPF นี้ ดูเหมือนว่าอยู่ในรูป oligomer และคงทนต่อการตัดย่อยด้วยเอนไซม์ trypsin พร้อมกันนี้พบว่าโปรตีน PPF ที่ได้ทำให้เกิดการขดตัวใหม่นี้สามารถทำให้เกิดการรั่วไหลของ glucose ที่ถูกใส่ไว้ใน liposomes จึงเสริมกับข้อสมมติฐานที่ว่า ชิ้นส่วน PPF ซึ่งประกอบด้วยเกลียวอัลฟาที่ 1-5 นั้น เป็นส่วนที่เกี่ยวข้องกับการทำให้เกิดรูรั่วของโปรตีนสารพิษดังกล่าว นอกจากนี้เราได้อาศัยวิธีการ single proline substitutions พบว่าการหักของเกลียวอัลฟาที่ 4 และ 5 มีผลกระทบโดยตรงกับความเป็นพิษฆ่าลูกน้ำยุง จึงเชื่อว่าเกลียวอัลฟาทั้ง 2 น่าจะเป็นองค์ประกอบที่สำคัญในการทำให้เกิดรูรั่วบนผนังเนื้อเยื่อ และได้ใช้วิธีการ charged to alanine mutagenesis ไปเปลี่ยนกรดอะมิโนที่มีประจุหรือมีขั้วไปเป็น alanine ในเกลียวอัลฟาที่ 4 อันได้แก่ Arg-143 Lys-156 Arg-158 Glu-159 และ Asn-151 พบว่า Arg-158 มีความสำคัญต่อความเป็นพิษของโปรตีนสารพิษ ซึ่งเมื่อนำข้อมูลนี้ไปใช้ร่วมกับวิธีการ Molecular Dynamics Simulations พบว่า รูรั่วจำลอง (pore model) ที่สร้างขึ้นในเนื้อเยื่อสังเคราะห์ที่มีน้ำร่วมอยู่ด้วยนั้น ซึ่งสร้างขึ้นจากเกลียวอัลฟาที่ 4 และ 5 (กรดอะมิโน Gln-140 ถึง Glu-198) ประกอบกันเป็น hexamers นั้น โดยที่ตำแหน่ง Arg-158 อยู่ทางด้านรูรั่วพบว่า ค่าการนำไฟฟ้า (conductance) ที่คำนวณได้นั้นให้ค่าขนาดของรูรั่วที่เกิดขึ้นมีส่วนเส้นผ่าศูนย์กลางประมาณ 2-3 นาโนเมตร

Keywords :

Bacillus thuringiensis, Delta-endotoxins, Inclusion Solubility, Refolding, Larvicidal Activity, Molecular Dynamics Simulations, Site-Directed Mutagenesis

Introduction

Bacillus thuringiensis (*Bt*) is a Gram-positive bacterium that has been used successfully as an alternative insecticide for biological control of disease vectors and other pests. During sporulation, different *Bt* strains produce larvicidal proteins in large quantities as cytoplasmic crystalline inclusions that are specifically toxic to a variety of dipteran, lepidopteran and coleopteran insect larvae [*1,2*]. These parasporal crystalline inclusions are composed of one or more polypeptides of varying molecular mass that have been classified as Cry and/or Cyt δ-endotoxins according to the similarity of their deduced amino acid sequences [*3,4*]. For instance, the 130-kDa mosquito-larvicidal protein from *Bt* subsp. *israelensis* is identified as the Cry4B toxin [*2,3*].

The general mechanism of gut epithelial cell disruption by the different *Bt* δ-endotoxins is evidenced to be the formation of lytic pores in the susceptible insect membrane [*5*]. When

ingested by susceptible larvae, the inclusions are solubilised by the alkaline pH of the larval midgut and the protoxins are activated by gut proteases. It is believed that the activated toxins then bind to midgut epithelial cells *via* specific receptors, and insert into the microvillar membrane to form ion channels or leakage pores that cause cell swelling and eventually death by colloid-osmotic lysis (see [*6*] for reviews). However, an entire characterisation at the molecular level of the pore-forming process mediated by these insecticidal proteins has not yet been obtained, although knowledge of how these insecticidal proteins function has increased substantially over the last decade.

The X-ray crystal structure of two different Cry toxins, the lepidopteran-specific Cry1Aa toxin [*7*] and the coleopteran-specific Cry3A toxin [*8*], reveals Cry proteins consisting of three distinct domains, and it is believed that each domain has a defined function including pore formation and receptor recognition [*7,8*]. Domain I is a group of seven α-helices in which the central helix (α5) is relatively hydrophobic and encircled by six other amphipathic helices. Domain II is the most variable part of the Cry toxin family and is composed of three anti-parallel β-sheets, each terminating in a surface-exposed loop. Domain III is a tightly packed β-sandwich of two anti-parallel sheets. It has been proposed that other members of this family will have the same overall tertiary structure since the core of the molecule including all the domain interfaces is built up from five amino acid sequence segments that are highly conserved throughout the entire Cry toxin family [*3,8*].

Structurally, it is immediately apparent that domain I is likely to be the transmembrane pore-forming apparatus. This domain contains five amphipathic helices (α3, α4, α5, α6 and α 7) that are theoretically long enough to span the bilayer lipid membrane and form a lytic pore [4,5]. The possibility that this α-helical bundle in domain I is essential for pore formation is supported by the feature that it is highly conserved in all Cry toxins [*3*], and by analogy with the helical bundle pore-forming structures of two other well-characterised bacterial toxins, colicin A and diphtheria toxin, although they bear no sequence homology [*9*]. This notion is further supported by several studies with truncated proteins corresponding to domain I of Cry1Ac [*10*] and Cry3B2 [*11*]. In addition, a number of studies *via* synthetic peptides or site-directed mutagenesis have provided evidence to support that α4 and α5 of several Cry toxins are involved in membrane penetration and pore formation [*12-18*].

Previously, we have found that in addition to removal of the C-terminal half of the 130-kDa Cry4B protoxin, the activated molecule had undergone proteolytic activation producing two main sets of cleavage products at ca. 47 kDa and ca. 21 kDa [*19*]. Aligning these positions with the Cry3A crystal structure [*8*] suggested that one cleavage occurred in a region before

the start of the N-terminal helical bundle and an other one occurred in a predicted loop joining helices 5 and 6 in the bundle [*20*]. This putative N-terminal five-helix bundle (α1-α5) was isolated as a protease-resistant fragment of ca. 21 kDa under denaturing conditions [*19*]. At present, the role of this α1-α5 fragment in the Cry4B mechanism of toxicity is still not clearly elucidated.

Experimental Procedures

Construction of the Plasmid Expressing the PPF Protein

A gene segment encoding the PPF (α1-α5) region (Met-1 to Leu-209; see Fig. 1) of the Cry4B toxin was generated by PCR using the plasmid template pMU388 containing the full-length 130-kDa Cry4B toxin gene [*21*]. Oligonucleotide primers (*universal primer*-f: 5'-TTGTGAGCGGATAACAATTTC-3'; *H5PPF*-r: 5'-GTGTACTGCACCATGGT**TTATTA**TAGTTGGT CACCAGA-3') were purchased from Genset Inc. (Singapore). The introduced *BamH*I site is underlined and two stop codons are shown as boldface. The PCR fragment with end-repaired *BamH*I-5' and *Nco*I-3' termini was directionally cloned into end-repaired *EcoR*I and *Nco*I sites of the expression vector pMEx8 containing the *tac* promoter [*22*], giving the recombinant plasmid pM4BH1-5. The PPF-coding sequence was verified by DNA sequencing using an ABI prism 377 sequencer.

Expression and Preparation of the PPF Protein

The PPF protein was over-expressed in *E. coli* strain JM109 by addition of isopropyl-β-D-thiogalactopyranoside (IPTG, 0.1 mM) to mid-exponential phase cultures, and partially purified as described earlier [*18*]. Protein concentrations were determined using a Bio-Rad protein quantitation kit, with bovine serum albumin fraction V (Sigma) as a standard. The protein inclusions (1 mg/ml) were solubilised at 37 ^{o}C for 1 hr in 50 mM Na_2CO_3 buffer, pH 9.0 supplemented with 6 M urea, and any insoluble protein was removed by centrifugation in a bench minifuge at 16,000×g for 15 min. The proteins was refolded by stepwise dialysis against 300 volumes of carbonate buffers with decreasing urea concentrations of 3 M, 1.5 M, 0.75 M, 0.5 M, 0.25 M and 0.1 M at 25°C for 2-3 hrs each, and finally dialysed twice against 300 volumes of carbonate buffer.

Proteolytic stability of the refolded PPF protein was analysed by digestion with 1:50 (w/w) trypsin [L-1-tosylamide-2-phenylethyl chloromethyl ketone (TPCK) treated, Sigma]: protein at 37 ^{o}C for 1 hr, and the samples were analysed by SDS 15% (w/v) PAGE. Immunoblotting was performed with polyclonal rabbit antibodies against the full length activated

Cry4B toxin. Immunocomplexes were detected with an anti-rabbit antibody-alkaline phosphatase conjugate (Sigma). An ABI 492 automated sequencer was used to determine N-terminal sequences of the electroblotted proteins on a polyvinylidene difluoride (PVDF) membrane (Problott, Applied Biosystems).

Construction of Mutant Toxin Plasmids

In vitro site-directed mutagenesis were performed using a Quickchange PCR-based mutagenesis kit (Stratagene) following the manufacturer's instructions. The plasmid pMU388 containing the full-length *cry4B* toxin gene [*21*] was used as a template. Complementary mutagenic oligonucleotides were purchased from Genset Inc. (Singapore). All mutations were verified by DNA sequencing using an ABI prism 377 sequencer.

Partial Purification and Solubilisation of Protoxin Inclusions

The wild type and mutant Cry4B toxin genes were expressed in *E. coli* strain JM109 under control of the *lac*Z promoter. Cells were grown in LB medium plus 100 µg/ml of ampicillin until OD_{600} reached 0.4-0.5 and incubation was continued for another 4 hrs after addition of IPTG to a final concentration of 0.1 mM. *E. coli* cultures expressing each mutant as inclusion bodies were harvested by centrifugation, resuspended in 1 ml of distilled water and then disrupted in a French Pressure Cell at 16,000 psi. The crude lysates were centrifuged at 8,000 *g* for 5 min and pellets obtained were washed 3 times in distilled water. Protoxin inclusions (1 mg/ml) were solubilised in 50 mM Na_2CO_3, pH 9.0 and incubated at 37 °C for 60 min as described previously [*18*]. After centrifugation for 10 min, the supernatants were analysed by SDS-15% (w/v) PAGE in comparison with the inclusion suspension. The solubilised protoxins were assessed for their proteolytic stability by digestion with TPCK treated) at a protoxin:trypsin ratio of 20:1 (w/w) for 16 hrs [*18*].

Liposome Entrapped Glucose Release Assays

Liposomes with trapped glucose were prepared by a modified method of Kinsky [*23*]. A lipid mixture (Sigma) of 12.5 µmole phosphatidylcholine (PC), 3.6 µmole dicetyl phosphate and 1.8 µmole cholesterol in 3 ml chloroform/methanol (2:1, v/v) was placed in a round bottomed flask and the solvent was removed under vacuum at 37°C. The resulting lipid film was resuspended in 0.5 ml of 300 mM glucose/ 10 mM HEPES, pH 8.0. Small unilamellar liposomes were prepared by squeezing the suspension through the extruder membrane (0.1 µ m in diameter, Avanti Polar Lipid) for a minimum of 11 passes. Unentrapped glucose was removed by gel filtration on a PD-10 column (Sephadex G-25, Pharmacia) equilibrated 150 mM

KCl/ 10 mM HEPES, pH 8.0. An aliquot of washed liposomes (100 nmole PC) was placed in a 1 ml disposable polymethyl methacrylate cuvette (Brand) containing 1 unit of hexokinase (Sigma), 1 unit of glucose-6-phosphate dehydrogenase (Sigma), 1 mM ATP, 0.5 mM NADP, 2mM Mg $(OAc)_2$ in 150 mM KCl/ 10 mM HEPES, pH 8.0. Glucose release, reflected as an increase in absorbance of NADPH at 340 nm, was monitored on an HP spectrophotometer. The relative glucose-release activities are indicated as fraction of maximum release which is defined as the amount release by 0.1% Triton X-100.

Mosquito-Larvicidal Assays

Larvicidal activity assays were performed as previously described [*18*] using 2-day old *Aedes aegypti* larvae reared from eggs supplied by the mosquito-rearing facility of the Institute of Molecular Biology and Genetics, Mahidol University, Thailand. About 500 larvae were reared in a container (22×30×10 cm deep) with approximately 3 l of distilled water supplemented with 0.2-0.3 g of rat diet pellets. In the assays, 1 ml of *E. coli* suspension (ca. 10^8 cells) was added to a 48-well microtitre plate (11.3 mm well diameter), with 10 larvae per well and a total of 100 larvae for each type of *E. coli* sample. *E. coli* cells containing the recombinant plasmid pMU388 and the pUC12 vector were used as positive and negative controls, respectively. Mortality was recorded after incubation for 24 hrs.

Molecular Dynamics Simulations

Coordinate of the putative transmembrane fragment (α4-α5) of Cry4B was obtained from the Cry4B homology model which has been constructed using the Cry3A crystal structure as a template (26). Models of pores formed by this helical hairpin were generated by simulated anneal/molecular dynamics (SA/MD) using Xplor V3.1 with the modified CHARMM PARAM 19 parameter set. Accessible surfaces of proteins were calculated by using Quanta V3.2 (Molecular Simulations). MD simulations on solvated model were performed using Gromacs 2.0 with the modified force field parameter set (30). Display and examinations of model were carried out using Rasmol and Insight II (Molecular Simulations). Computations were performed om SGI Indigo, Cray 2000 or Linux/Intel Pentium II. Diagrams of structures were drawn using Molscript. Helix crossing angels, hilix-membrane tilting angle and interhelical distances were determines with routines, written for Gromacs 2.0. Pore dimension and elestrostatic potential along axis were determined by using HOLE 2.0.

Results and Discussion

Expression and Characterisation of the α1-α5 PPF Fragment

In the preliminary experiments, the results of size-exclusion FPLC analysis under non-denaturing conditions (carbonate buffer, pH 9.0) indicated that the 21-kDa N-terminal helix bundle (α1-α5) of the Cry4B toxin remains non-covalently associated with the C-terminal portion (ca. 47 kDa) of the activated toxin after proteolytic activation with trypsin (Angsuthanasombat, C., unpublished data). Attempts were made to isolate this α1-α5 fragment by FPLC under denaturing conditions (8 M urea, carbonate buffer, pH 9.0) were unsuccessful. In this study, cloning of the PPF fragment in *E. coli* and over-expression of the protein allowed the isolation and biochemical characterisation of this PPF protein.

Upon induction with IPTG, *E. coli* cells harbouring the plasmid clone (pM4BH1-5) expressed the PPF protein at high levels in the form of sedimentable inclusion bodies with a yield of approximately 15 mg per liter of culture (see Fig. 2A). Analysis of the inclusion preparation by SDS-PAGE revealed a major band at 23 kDa which specifically cross-reacted in Western blots probed with antibodies raised against the activated Cry4B toxin (Fig. 2B). The N-terminal sequence of the 23-kDa protein obtained by automated Edman degradation was found to be identical to the N-terminus of the 130-kDa protoxin (MNSGY...). Since the predicted molecular mass of the polypeptide encoded in the cloned PPF fragment is 23.587 kDa, these results provide evidence that the 23-kDa product we have obtained from over-expressing *E. coli* corresponds to the N-terminal α1-α5 segment of the Cry4B toxin.

Unlike the inclusions of the full length protoxin (1 mg/ml) which are soluble (up to 80%) in carbonate buffer, pH 9.0 (*18*), the PPF inclusions (1 mg/ml) were readily soluble only in the presence of 6 M urea, giving at least 60% solubility (see Fig. 3). The PPF protein was refolded by stepwise dialysis against buffers with decreasing urea concentrations and finally the protein was obtained in urea-free carbonate buffer, pH 9.0 at a concentration of ?? mg/ml. The refold PPF preparation (Fig. 3, lane 3) was subjected to size-exclusion FPLC using a Superose 12 column (Pharmacia) with carbonate buffer, pH 9.0 as eluent at a flow rate of ?? ml/min. Elution of the protein was monitored at 280 nm and the 23-kDa PPF protein apparently was eluted in the void volume of the column (data not shown). This suggested that the presence of a high molecular mass (> 300 kDa) oligomer or aggregate rather than a monomeric form of the refolded PPF protein. Notwithstanding this observation, this aggregate could represent a stable and functional oligomerisation state of the PPF fragment with the ability to intercalate into lipid membranes to form a pore. Interestingly, treatment of the refolded 23-kDa PPF protein with trypsin resulted in a 21-kDa protein fragment detectable by

SDS-PAGE (see Fig. 3, lane 4) and specifically cross-reacted with Cry4B toxin antibodies (data not shown). We conclude that this 21-kDa PPF protein is structurally resistant to further proteolysis and that the refolded 23-kDa PPF protein likely exists in its native folded conformation. Proteins which are extensively resistant to proteolysis have been shown to maintain a significant portion of native-like conformation [*24*].

No significant activity was observed in bioassays against *A. aegypti* larvae using *E. coli* cells expressing the PPF protein. Lack of toxicity is most likely due the absence of a three-β-sheet domain [*8*] which is required for binding of the activated toxin to larval midgut epithelial cells *via* specific receptors. It is still an open question whether after proteolytic activation *in vivo*, the bundle of five helices remains associated with the 47-kDa fragment containing the receptor-binding domain in the pore-forming process. In other studies with the Cry4A cleavage products genetically fused with glulathione S-transferase (GST), significant larvicidal activity was observed only when both of the fusion proteins, GST-20-kDa (α1-α5) and GST-45-kDa containing the receptor-binding domain, were co-ingested by the larvae [*25*].

The membrane lytic capability of the refolded PPF protein was assayed a glucose release assay using receptor-free phospholipid vesicles. Under the conditions used in this assay, the refolded PPF fragment (15 µg/ml) was able to induce release of entrapped glucose from liposomes (see Fig. 4). Approximately 77% of maximum release activity (when compared to Triton X-100 as positive control) was observed within 10 min after addition of the protein. However, the full length activated Cry4B toxin gave ca. 65% maximum release at a concentration of 45 µg/ml whereas the 130-kDa Cry4B protoxin (90 µg/ml) and a control sample containing carbonate buffer, pH 9 showed only little release (< 20%). These results are consistent with former findings that the N-terminal α-helical bundles of the Cry1Ac and Cry3B2 toxins were able to mediate the release ^{86}Rb cation from phospholipid vesicles and form cation selective channels in planar lipid bilayers [*10,11*].

In summary, our results demonstrate that the 23-kDa α1-α5 fragment is fully capable of permeabilising the membrane liposomes *in vitro* apart from the rest of the activated Cry4B toxin, and therefore constitutes the region responsible for membrane insertion and pore formation within the Cry toxin molecules. The cloned PPF fragment will facilitate further investigations on the pore-forming mechanism of the Cry insecticidal toxins.

Proline Substitutions of Selected Helices Affect Toxin Solubility and Toxicity

we have made use of PCR-based mutagenesis to construct several more mutants in the putative pore-forming domain to determine which of the three other helices (α5, α6 or α7) would be responsible for toxicity of the mosquito-active Cry4B toxin. Proline substituted

mutants were designed based on a 3D Cry4B model which was previously constructed by homology modelling using Cry3A as a template [*26*]. The designed mutants have single proline substitutions in the central region of the selected helices of Cry4B including α5 at residues Val-181, Ala-182 and Leu-186, α6 at Gln-215 and α7 at Thr-254 (Fig. 5). Each mutant gene could be over-expressed in *E. coli* under inducible control of the *lac*Z promoter and the mutant toxins were predominantly produced as sedimentable inclusion bodies which were then partially purified. In addition, the level of protein expression of all mutant proteins was approximately the same as that of the wild type, and the expressed mutant derivatives still cross-reacted with Cry4B antibodies (data not shown).

Experiments were carried out to assess the solubility of mutant protein inclusions in carbonate buffer, pH 9.0 in comparison with that of the wild-type inclusion. The amounts of the 130-kDa soluble proteins in the supernatant were compared with those of the proteins initially used in order to determine the percentage of protein solubilisation. A complete loss of solubility at alkaline pH was observed for the inclusions of the mutants substituted in α5, α6 or α7, whilst the inclusions of the two previously constructed mutants, V118P and Q149P, exhibited the same solubility characteristics as that of the wild-type (Fig. 6). The reason for the difference in solubility between those two sets of point mutations is not clear. However, this may be explained by the fact that all the five mutated residues, *i.e.* Val-181, Ala-182 and Leu-186 in α5, Gln-215 in α6 and Thr-254 in α7 are buried in the protein core, unlike Val-118 in α 3 and Gln-149 in α4 that are exposed at the protein surface (see Fig. 5C). Thus, the bend created by the proline substitution in these relatively conserved helices, *i.e.* α5, α6 or α7 possibly disturbs the structural characteristics either locally or globally that might consequently affect inclusion formation as demonstrated by a drastically perturbed dissolvability. On the other hand, the proline mutations in α3 or α4 appear to affect only the individual helices, without significantly influencing the other helices or the overall structure, as earlier demonstrated for an α-lactalbumin folding intermediate [*27*].

To determine whether a single proline replacement in these three additional helices also affects the larvicidal activity of Cry4B, *E. coli* cells expressing each type of the mutant toxins were bioassayed using *A. aegypti* mosquito-larvae (Fig. 7). The mortality data recorded after a 24-hr incubation reveals that the α6 mutant (Q215P) still exhibited full larvicidal activity (98.7±0.7%) similar to the α3 mutant (V118P), whereas the T254P mutant produced merely 23.7±13.9%. However, mortality of all the α5 mutants, V181P, A182P and L186P, was almost totally abolished as approximately comparable to that observed with the previously described α

4 mutant (Q149P). These results suggest that the integrity of α5 and α7 may indeed be important for toxin activity like that of α4.

Although toxin inclusion insolubility and larvicidal activity are seemingly correlated for all the three α5 mutants and the α7 mutant, the insolubility *in vitro* may not always necessarily reflect toxin activity *in vivo* as observed for the α6 mutant which was insoluble at pH 9.0 but still bioactive. It has been previously demonstrated that the difference detected in solubilisation *in vitro* for Cry4A inclusions which were purified from two different *Bt* recipient strains, is not a factor in larval toxicity [*28*]. Presumably, larval midgut proteases *in vivo* might facilitate the dissolution of the ingested toxin inclusions which would negate the differences between the observed toxicities of the α3 and α6 mutants. It was shown that incubation of the Cry2A toxin with gut proteases enhanced the solubility of the toxin inclusion, obviating the requirement for reducing agents at pH10.5 [*29*].

In conclusion, this report additionally demonstrates that the central helix (α5), α6 and α7, but not α3 or α4, are conceivably involved in protein packing for inclusion formation, thus destabilising these three helices individually could gives rise to toxin insolubility *in vitro*. Moreover, our study also provides further support for a crucial role of the pore-forming helical hairpin α4-α5 as well as α7, which has been suggested to be a domain binding sensor [*13*], in larvicidal activity of the Cry4B toxin.

Charged Residue Screening in α4 Reveals One Critical residue for Toxicity

As predicted from the homology-based model of Cry4B [*26*], helix 4 is composed of 26 amino acids of which four are charged (see Fig. 8A). These charged residues, Arg-143, Lys-156, Arg-158 and Glu-159, are widely distributed along the hydrophilic surface (Fig. 8B). In the present study, five Cry4B mutants, R143A, N151A, K156A, R158A and E159A, were generated at five different positions (see Fig. 8C) by substituting each relevant residue with alanine *via* PCR-based mutagenesis. The energy-minimised models for these mutants suggested that each point mutation would not cause drastic changes in the overall structure of the mutant toxins.

Upon induction with IPTG, *E. coli* cells transformed with each mutant plasmid highly expressed the 130-kDa Cry4B derivatives as inclusion bodies with a yield comparable to the wild-type toxin. After partial purification, protein preparations were analysed by SDS-PAGE and all shown to contain more than 90% pure Cry proteins (Fig. 9, lanes 2,4,6,8, 10 and 12). In addition, all mutant protein inclusions were found to be soluble in carbonate buffer, pH 9.0, giving at least 70% solubility which resembles closely the wild-type inclusions under similar conditions [*18*]. The solubilised mutant protoxins were also examined for their proteolytic

stability by digestion with trypsin and all found to produce protease-resistant products of ca. 47 and ca. 21 kDa identical to the wild-type protoxin (Fig. 9, lanes 3,5,7,9,11 and 13) [*21*]. These results suggested that all the mutant protoxins containing alanine substitutions had folded to their native conformation.

E. coli cells expressing each type of the mutant toxin were tested for their relative toxicity against *Aedes aegypti*. All assays were carried out in ten replicas for each sample and repeated three times; the mortality data recorded after a 24-hr incubation are shown in Fig. 10. Compared with wild-type Cry4B, four mutants with alanine substitutions at charged residues (Arg-143, Lys-156 and Glu-159) or at one polar residue (Asn-151) exhibited no loss of larvicidal activity. In contrast, one mutant with the alteration of a charged amino acid at Arg-158 was not active against the larvae.

As suggested by solubilisation and trypsin activation of the Cry4B protoxin, the mutations did not induce structural distortions in the toxin molecule. Therefore, the complete loss of toxicity observed for the R158A mutant is least likely to be caused by misfolding of the protein. Considered as a whole, our results indicate that the side of helix 4 containing Arg-158 is an important determinant for larvicidal activity of the Cry4B toxin. This notion is supported by experimental results obtained with directed substitutions of helix 4 residues in other Cry proteins, Cry1Aa and Cry1Ac [*16,17*].

Recently, Masson *et al.* [*17*] have constructed a series of charged residue mutants in helix 4 of the Cry1Aa toxin. The mutant toxins were tested for toxicity against *Plutella xylostella* diamondback moth larvae and found that mutants with alterations at Glu-129, Arg-131 or Asp-136 showed a complete loss of larvicidal activity. Based on conductance experiments with planar lipid bilayers, the authors have concluded that loss of toxicity was caused by prevention of formation of ion channels in these mutants and that the negative charge of Asp-136 and Glu-129 contributes directly to the passage of ions through the transmembrane pore. Interestingly, their positively charged non-toxic mutant R131Q displayed reduced conductance, albeit the structural basis for this observation is not clear yet. For the Cry1Ac toxin, the R131L substitution has been shown to cause a 10-fold reduction in toxicity against *Manduca sexta* tobacco hornworm [*16*]. We have recently constructed a homology model for the Cry4B toxin [*26*] in which Arg-158 is located on the same side of helix 4 relative to Arg-131 in the Cry1Aa toxin [*7*] (see Fig. 8B&C). Despite a relatively high degree of similarity in both structures, our experiment revealed that elimination of the only negatively charged side chain in helix 4, Glu-159, which corresponds to Asp-136 in Cry1Aa (Fig. 8C), did not affect toxin activity of Cry4B. It is conceivable that these differences in response to

modification of charged residues reflect subclass-specific variations in the channel architecture for individual Cry proteins. Further experimentation is required to answer the question whether alanine substitutions at Arg-158 and Glu-159 are conducive to alterations in the passage of ions through the pore.

Molecular Dynamics Simulation of the α4-α5 Hairpin

The putative transmembrane fragment (α4-α5) remained as a helix-turn-helix hairpin motif in POPC/water system during 1 ns molecular dynamics simulations (Fig. 11). Relaxing of helical structure at C-terminal of α5 was observed. Thickness of POPC region did not show any signification change during 1 ns unrestrained molecular dynamics simulations. α4 and α5 tilting angle remained 19.39 ± 1.68 and 4.42 ± 1.50 degree, respectively. In addition, α4-α5 crossing angle remained 15.74 ± 0.83 degree (Fig. 12).

Heavy fluctuations of Cα atoms were found loop region (Asn166-Glu171) (Fig. 13). Milder fluctuations were at the middle of α4 (L157-T160) and both termini of the peptide. The fluctuations at middle of α4 might be due to unsatisfied properties of the polar residues (K156, R158, E159 and T160) in this region. Only few interhelical hydrogen bonds were detected but no any salt-bridge was found in the model. Similar to other transmembrane peptides, the pore model composing α4-α5 showed peptide/water hydrogen at residues which are exposing to water, suggesting that the hairpin might be mostly stabilized by hydrophobic interaction between α4 and α5 and the organisation of the peptides in lipid bilayers would be stabilized by protein/water interaction near lipid/water interface. The results also suggested that the α4-α5 fragment has high potential to form a stable helical hairpin in lipid/water system. Predicted conductance values suggested that the transmembrane α4-α5 hairpin of Cry4B has a potential to form a stable oligemeric pore with 2-3 nm in diameter that is consistent with the observed cation permeability of the Cry4B toxin ion channels. Such pore diameter calculations also demonstrate that rings of pore-lining residues contribute a series of contrictions along the pore.

References

1 Aronson, A.I., Beckman, W. and Dunn, P. (1986) *Bacillus thuringiensis* and related insect pathogens. *Microbiol. Rev.* **50**, 1-24.

2 Schnepf, E., Crickmore, N., Van Rie, J., Lereclus, D., Baum, J., Feitelson, J., Zeigler, D.R. and Dean, D.H. (1998) *Bacillus thuringiensis* and its pesticidal crystal proteins. *Microbiol. Mol. Biol. Rev.* **62**, 775-806.

3 Hofte, H. and Whiteley H.R. (1989) Insecticidal crystal proteins of *Bacillus thuringiensis*. *Microbiol. Rev.* **53**, 242-255.

4 Crickmore, N., Zeigler, D.R., Feitelson, I., Schnepf, E., Van Rie, J., Lereclus, D., Baum, J. and Dean, D.H. (1998) Revision of the nomenclature for the *Bacillus thuringiensis* pesticidal crystal proteins. *Microbiol. Mol. Biol. Rev.* **62**, 807-813.

5 Knowles, B.H. and Ellar, D.J. (1987) Colloid-osmotic lysis is a general feature of the mechanism of action of *Bacillus thuringiensis* δ-endotoxins with different insect specificity. *Biochem. Biophys. Acta.* **924**, 509-518.

6 Knowles, B.H. (1994) Mechanism of action of *Bacillus thuringiensis* insecticidal δ-endotoxins. *Adv. Insect Physiol.* **24**, 275-308.

7 Grochulski, P., Masson, L., Borisova, S., Pusztai-Carey, M., Schwartz, J.L., Brousseau R. and Cygler, M. (1995) *Bacillus thuringiensis* CryIA(a) insecticidal toxin: crystal structure and channel formation. *J. Mol. Biol.* **254**, 447-464.

8 Li, J., Carroll, J. and Ellar, D.J. (1991) Crystal structure of insecticidal delta-endotoxin *from Bacillus thuringiensis* at 2.5 Å resolution. *Nature* **353**, 815-821.

9 Parker, M.W. and Pattus, F. (1993) Rendering a membrane protein soluble in water: a common packing motif in bacterial protein toxins. *Trends Biochem. Sci.* **18**, 391-395.

10 Walters, F.S., Slatin, S.L., Kulesza, C.A. and English, L.H. (1993) Ion channel activity of N-terminal fragments from CryIA(c) delta-endotoxin. *Biochem. Biophys. Res. Commun..* **196**, 921-926.

11 Von Tersch, M.A., Slatin, S.L., Kulesza, C.A. and English, L.H. (1994) Membrane-permeabilizing activities of *Bacillus thuringiensis* coleopteran-active toxin CryIIIB2 and CryIIIB2 domain I peptide. *Appl. Environ. Microbiol.* **60**, 3711-3717.

12 Cummings, C.E., Armstrong, G., Hodgman, T.C. and Ellar, D.J. (1994) Structural and functional studies of a synthetic peptide mimicking a proposed membrane inserting region of a *Bacillus thuringiensis* delta-endotoxin. *Mol. Membr. Biol.* **11**, 87-92.

13 Gazit, E., La Rocca, P., Sansom, M.S.P. and Shai, Y. (1998) The structure and organization within the membrane of the helices composing the pore-forming domain of *Bacillus thuringiensis* delta-endotoxin are consistent with an "umbrella-like" structure of the pore. *Proc. Natl. Acad. Sci. USA* **95**, 12289-12294.

14 Gerber, D. and Shai, Y. (2000) Insertion and organization within membranes of the delta-endotoxin pore-forming domain, helix 4-loop-helix 5, and inhibition of its activity by a mutant helix 4 peptide. *J. Biol. Chem.* (in press)

15 Schwartz, J.L., Juteau, M., Grochulski, P., Cygler, M., Prefontaine, G., Brousseau, R. and Masson, L. (1997) Restriction of intramolecular movements within the Cry1Aa toxin molecule of *Bacillus thuringiensis* through disulfide bond engineering. *FEBS Lett.* **410**, 397-402.

16 Kumar, A.S. and Aronson, A.I. (1999) Analysis of mutations in the pore-forming region essential for insecticidal activity of a *Bacillus thuringiensis* delta-endotoxin. *J. Bacteriol.* **181**, 6103-6107.

17 Masson, L., Tabashnik, B.E., Liu, Y.B., Brousseau, R. and Schwartz, J.L. (1999) Helix 4 of the *Bacillus thuringiensis* Cry1Aa toxin lines the lumen of the ion channel. *J. Biol. Chem.* **274**, 31996-32000.

18 Uawithya, P., Tuntitippawan, T., Katzenmeier, G., Panyim, S. and Angsuthanasombat, C. (1998) Effects on larvicidal activity of single proline substitutions in α3 or α4 of the *Bacillus thuringiensis* Cry4B toxin. *Biochem. Mol. Biol. Inter.* **44**: 825-832.

19 Angsuthanasombat, C., Crickmore, N. and Ellar, D.J. (1991) Cytotoxicity of a cloned *Bacillus thuringiensis* subsp. *israelensis* CryIVB toxin to an *Aedes aegypti* cell line. *FEMS Microbiol. Lett.* **83**, 273-276.

20 Angsuthanasombat, C., Crickmore, N. and Ellar, D.J. (1993) Effects on toxicity of eliminating a cleavage site in a predicted interhelical loop in the *Bacillus thuringiensis* CryIVB δ-endotoxins. *FEMS Microbiol. Lett.* **111**, 255-262.

21 Angsuthanasombat, C., Chungjatupornchai, W., Kertbundit, S., Luxananil, P., Settasatian, C., Wilairat, P. and Panyim, S. (1987) Cloning and expression of 130-kd mosquito-larvicidal delta-endotoxin gene of *Bacillus thuringiensis* var. *israelensis* in *Escherichia coli*. *Mol. Gen. Genet.* **208**, 384-389.

22 Buttcher, V., Ruhlmann, A. and Cramer, F. (1990) Improved single-stranded DNA producing expression vectors for protein manipulation in *Escherichia coli*. *Nucleic Acids Res.* **18**, 1075.

23 Kinsky, S.C. (1974) Preparation of liposomes and a spectrophotometric assay for the release of trapped glucose marker. *Meth. Enzymol.* **32**, 501-513.

24 Fontana, A., Polverino de Laureto, P., De Filippis, V., Scaramella, E. and Zambonin, M. (1997) Probing the partly folded states of proteins by limited proteolysis. *Folding & Design.* **2**, R17-R26.

25 Yamagiwa, M., Esaki, M., Otake, K., Inagaki, M., Komano, T., Amachi, T. and Sakai, H. (1999) Activation process of dipteran-specific insecticidal protein produced by *Bacillus thuringiensis* subsp. *israelensis*. *Appl. Environ. Microbiol.* **65**, 3464-3469.

26 Uawithya, P., Krittanai, C., Katzenmeier, G., Leetachewa, S., Panyim, S. and Angsuthanasombat, C. (1999) 3D models for *Bacillus thuringiensis* Cry4A and Cry4B insecticidal proteins based on homology modelling. Abstract 32nd Meeting, Society for Invertebrate Pathology, Irvine, USA, p.75.

27 Schulman, B.A. and Kim, P.S. (1996) Proline scanning mutagenesis of a molten globule reveals non-cooperative formation of a protein's overall topology. *Nature Struct. Biol.* **3**, 682-687.

28 Angsuthanasombat, C., Crickmore, N. and Ellar D.J. (1992) Comparison of *Bacillus thuringiensis* subsp. *israelensis* CryIVA and CryIVB cloned toxins reveals synergism *in vivo*. *FEMS Microbiol. Lett.* **94**, 63-68.

29 Nicholls, C.N., Ahmad, W. and Ellar, D.J. (1989) Evidence for two different types of insecticidal P2 toxins with dual specificity in *Bacillus thuringiensis* subspecies. *J. Bacteriol.* **171**, 5141-5147.

30 Keer, I.D., Sankararamakrishnan, R., Breed, J. and Sansom, M.S.P. (2000) Molecular modelling of staphylococcal δ-toxin ion channels by restrained molecular dynamics. *Prot. Engineer.* (in press).

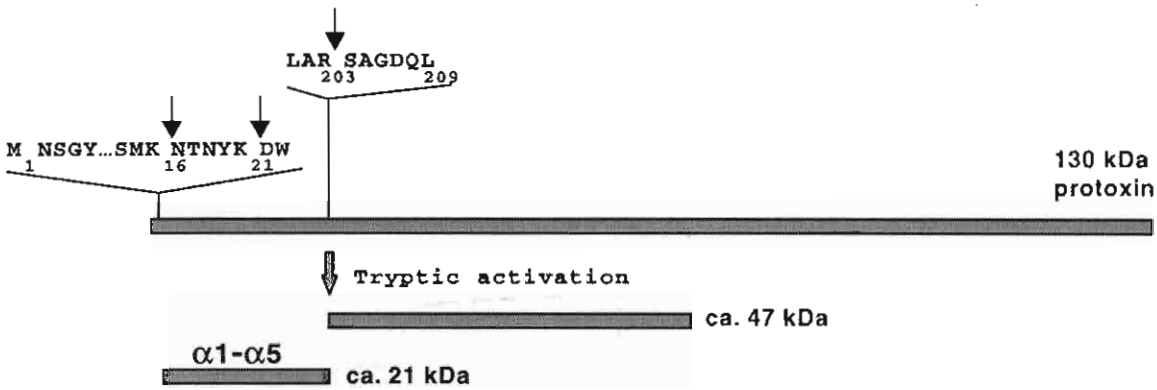

FIGUTURE 1 Tryptic processing of the 130-kDa Cry4B protoxin. An overview of the results obtained from N-terminal sequencing of trypsin-treated products of Cry4B. The arrows indicate the known cleavage sites within the toxin. The region between Met-1 and Leu-209 represent the PPF fragment.

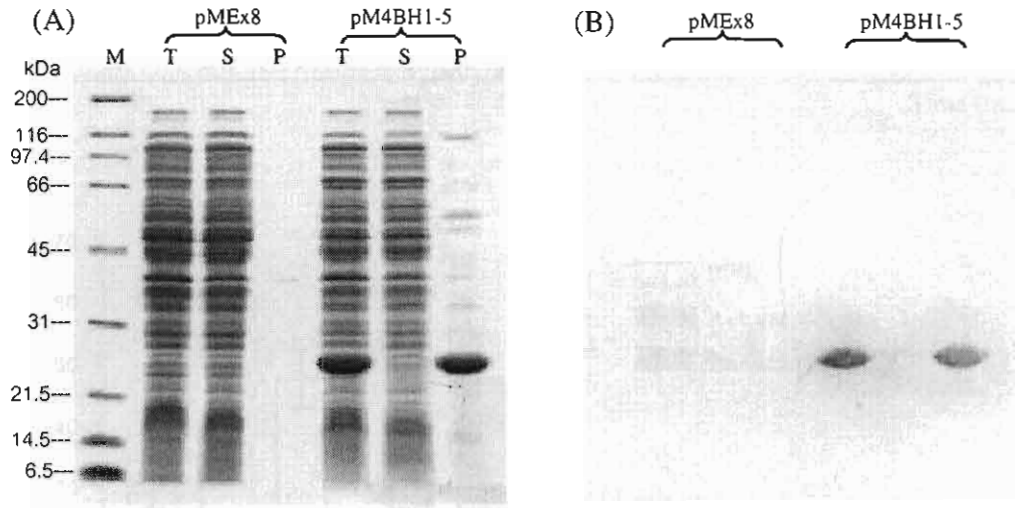

FIGURE 2 Expression of the PPF protein in *E. coli*. (A): A Coomassie brilliant blue-strained SDS-15 % polyacrylamide gel showing the total crude extracts (T) of *E. coli* cells harbouring the pMEx8 vector or the pM4BH1-5 recombinant encoding the PPF protein. (B): Immunoblot analysis of (A) showing the 23-kDa PPF protein cross-reacted with Cry4B antibodies. (M) represents molecular mass standards. (S) and (P) are the supernatant and pellet fractions,

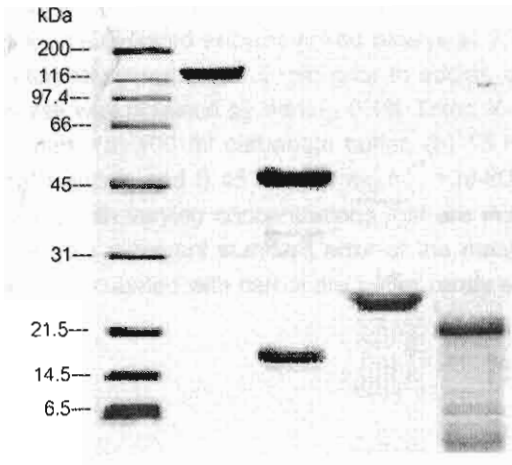

FIGURE 3 SDS-PAGE (15% gel) analysis of tryptic processing of Cry4B and the PPF protein. M represents molecular mass standards. Lane 1 is the 130-kDa solubilised protoxin. Lane 2 is the activated toxin. Lanes 3 and 4 are refolded PPF and the refolded protein treated with trypsin (1:50 enzyme:protein, w/w), respectively.

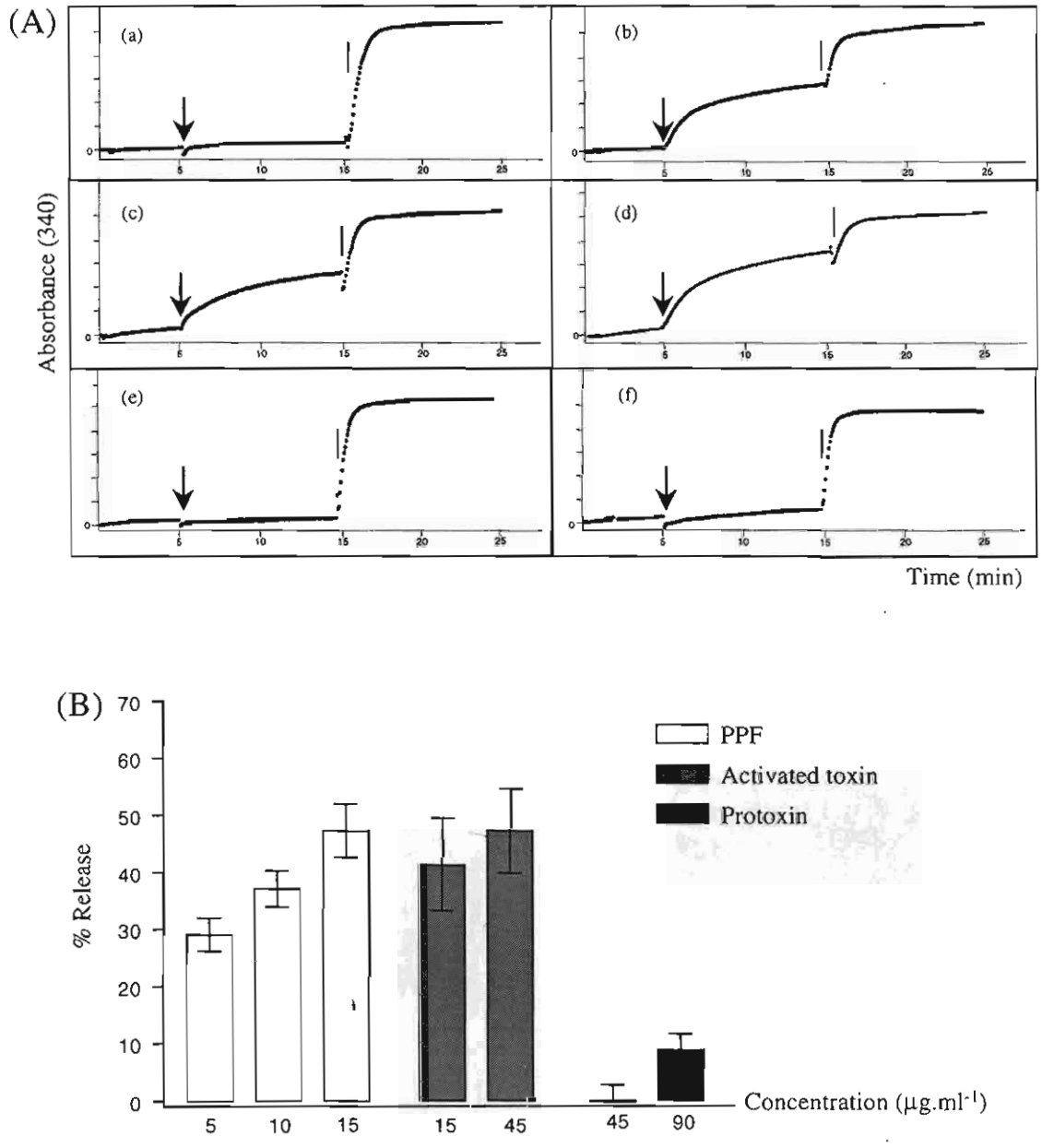

FIGURE 4 Effect on glucose release from liposomes. (A): Release of entrapped glucose was monitored by using NADP-linked enzyme-linked assays at 25 °C. The traces represent absorbance at 340 nm which was continously recorded for 5 min prior to adding each protein sample as indicated by an arrow. The maximum release was obtained by adding 0.1% Triton X-100 (indicated by a vertical bar) after 10 min incubation with samples; (a) 100 ml carbanate buffer, (b) 15 $mg.ml^{-1}$ refolded PPF, (c and d) 15 and 45 $mg.ml^{-1}$ activated Cry4B and (e and f) 45 and 90 $mg.ml^{-1}$ 130-kDa protoxin. (B): The relative release activities of each protein sample with varying concentrations that are indicated as fraction of 100% release induced by Triton X-100. Error bars represent standard error of the mean from five separate experiments. The release in the control sample incubated with carbonate buffer rarely exceeded 10% and these values have been subtracted in the figure.

A)

α3 α4

Cry3A 123 DYAKNKALAELQGLQNNVEDYVSALSSWQKNPVSSRNPHSQGRIRELFSQAESHFRNSMPSFA-ISGY

Cry4B 106 AYVRTDANAKMT**V**VKDYLDQYTTKFNTWKREPN---NQSYRTAVIT**Q**FNLTSAKLRETAVYFSNLVGY

118 149

α5 α6

Cry3A 190 EVLFLTTYAQAANTHLFLLKDAQIYGEEWGYEKEDIAEFYKRQLKLTQEYTDHCVKWYNVGLDKLRGS

Cry4B 171 ELLLLPIYA**Q**VANFN**L**LLIRDGLINAQEWSLARSAGDQLYNTMV**Q**YTKEYIAHSITWYNKGLDVLRNK

181 186 215

182

α7

Cry3A 258 SYESWVNFNRYRREMTLTVLDLIALFPLYDVRL

Cry4B 239 SNGQWITFNDYKREM**T**IQVLDILALFASYDPRR

254

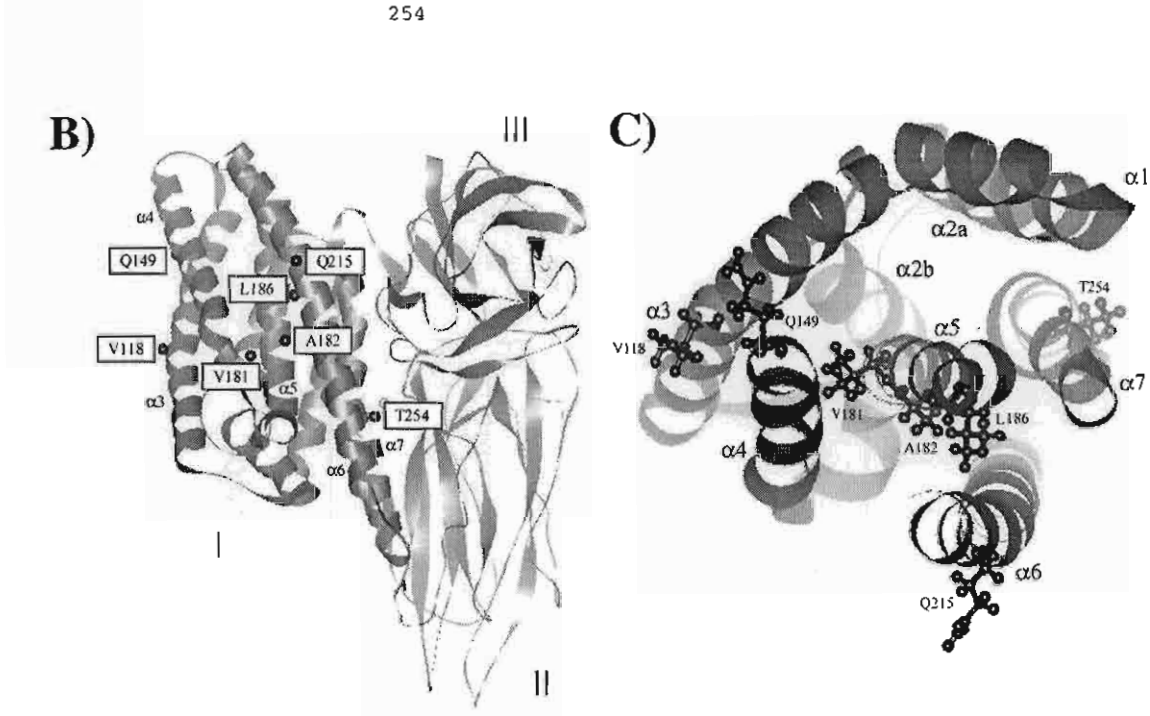

FIGURE 5 **A)** Amino acid sequence alignment of Cry4B with the known secondary structure elements of Cry3A. Single proline substitutions at each indicated position are underlined and emboldened. The corresponding helices are shown above the sequences. **B)** A ribbon representation (generated by Weblab viewer, Molecular Simulation Inc.) of the Cry4B model built by homology modelling [*26*], illustrating the three-domain organisation (I-III). Black beads indicate β-carbon atoms of the mutated residues. **C)** Top view of the helical bundle in domain I of Cry4B. The mutated residues are shown as ball and stick: α3 at Val-118, α4 at Gln-149, α5 at Val-181, Ala-182, and Leu-186, α6 at Gln-215 and α7 at Thr-254.

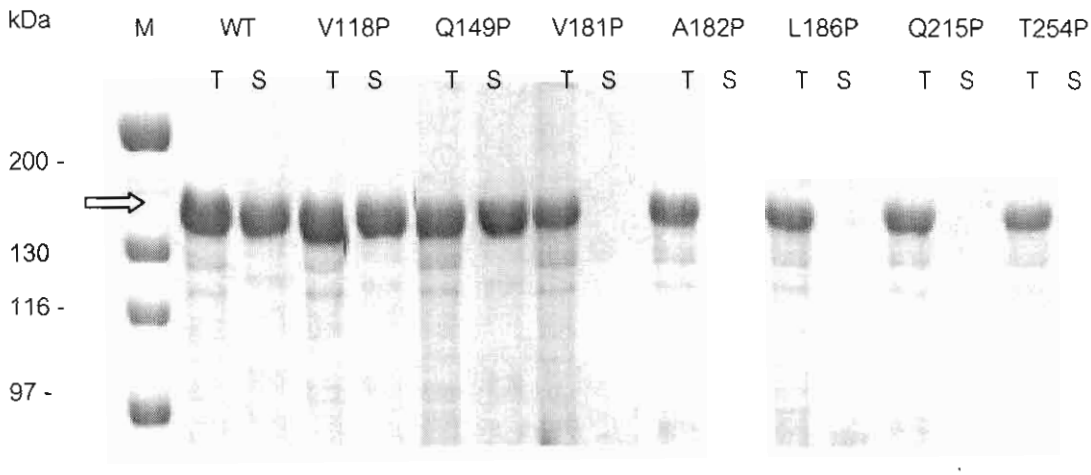

FIGURE 6 The figure shows a Coomasie brilliant blue-stained SDS-15% polyacrylamide gel of the partially purified 130-kDa protein inclusions extracted from *E. coli* expressing the wild-type (WT) and mutant Cry4B toxins and solubilised in carbonate buffer. (T) and (S) represent the total fractions and an equivalent volume of the supernatants after centrifugation, respectively. (M) represents the molecular mass standards.

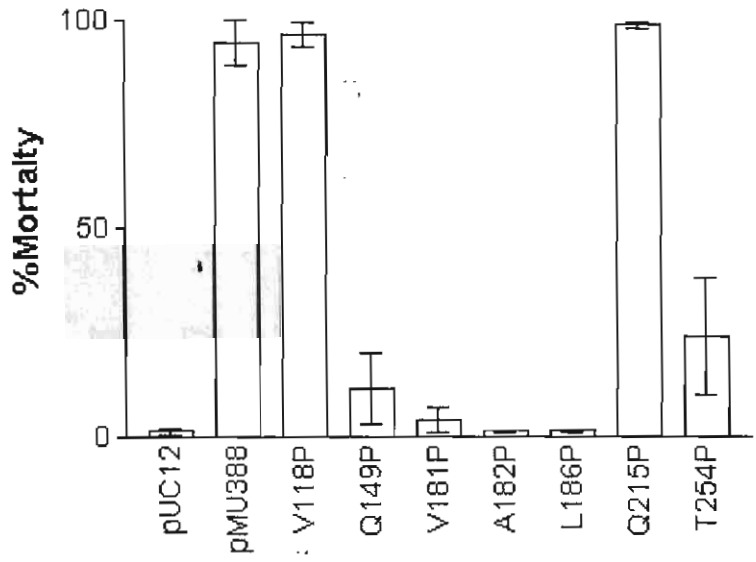

FIGURE 7 Lavicidal activities of *E. coli* cells expressing either the Cry4B wild-type toxin (pMU388) and its mutants (V118P, Q149P, V181P, A182P, L186P, Q215P and T254P) against *A. aegypti* larvae. Error bars indicate standard error of the mean from three independent experiments

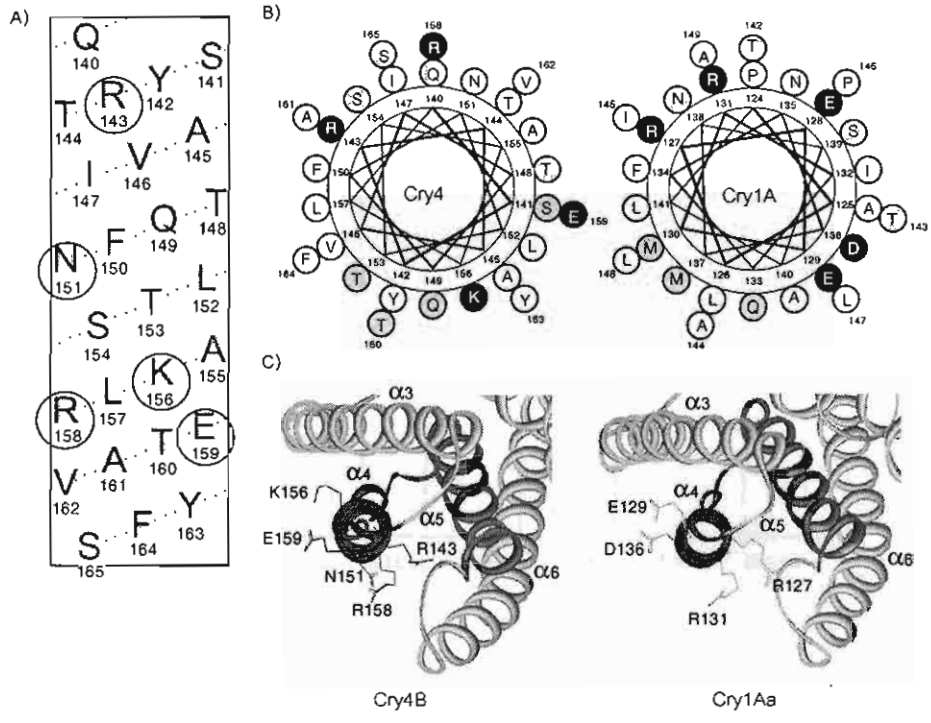

FIGURE 8 (A): A predicted pattern of helix 4 of Cry4B redrawn from [20] is composed of 26 residues of which the encircled residues were substituted by alanine. (B): Helical wheel projections of helix 4 of Cry4B and Cry1Aa. Amino acid residues are plotted every 100 degrees consecutive around the wheel, following the sequences given in A and [15] for Cry4B and Cry1Aa, respectively. The following colour code is used: black is an amino acid with a charged side chain; gray is a polar side chain and white is a hydrophobic side chain. (C): Top views of amino acid arrangement in helix 4 together with the relative positions of helices 3, 5 and 6 in a 3D Cry4B model built by homology modelling [21] and the Cry1Aa structure [7]. The labeled residues indicate the targeted positions. The structures were prepared using Weblab viewer (Molecular Simulation Inc.).

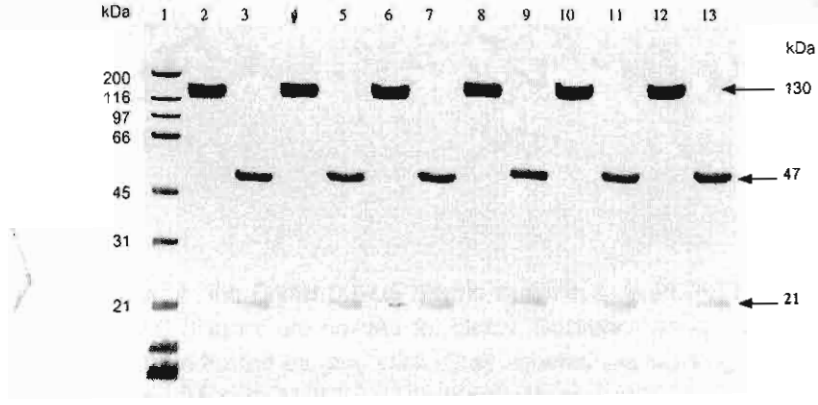

FIGURE 9 Coomassie brilliant blue-stained SDS-15% polyacrylamide gel comparing the yields of solubilised protoxins and their trypsin-cleavage products. Lane 1 represents molecular mass standards. Lanes 2, 4, 6, 8, 10 and 12 are the solubilised 130-kDa Cry4B protein and its mutant protoxins R143A, N151A, K156A, R158A and E159A, respectively. Lanes 3, 5, 7, 9, 11 and 13 are trypsin-cleavage products of the above samples run in the same order.

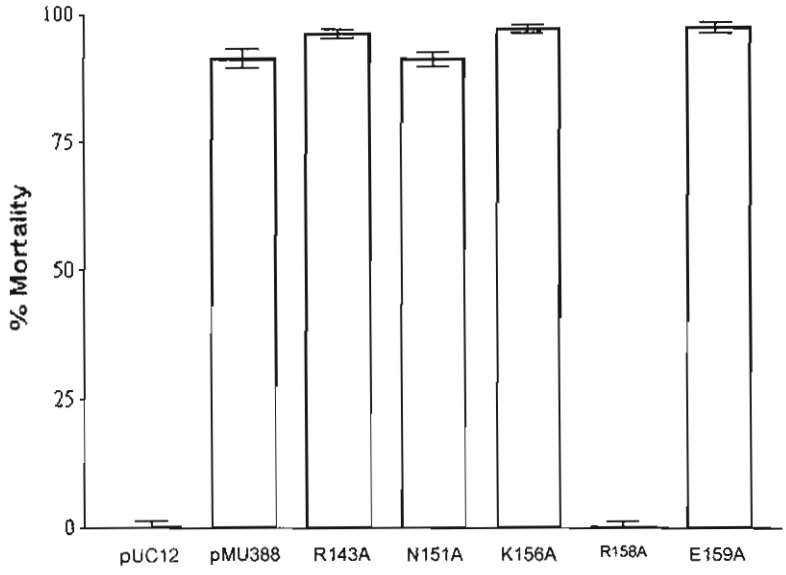

FIGURE 10 Mosquito-larvicidal activities of *E. coli* cells expressing the Cry4B wild-type toxin (pMU388) or its mutants (R143A, N151A, K156A, R158A and E159A) against *Aedes aegypti* larvae. Error bars indicate standard error of the mean from three independent experiments.

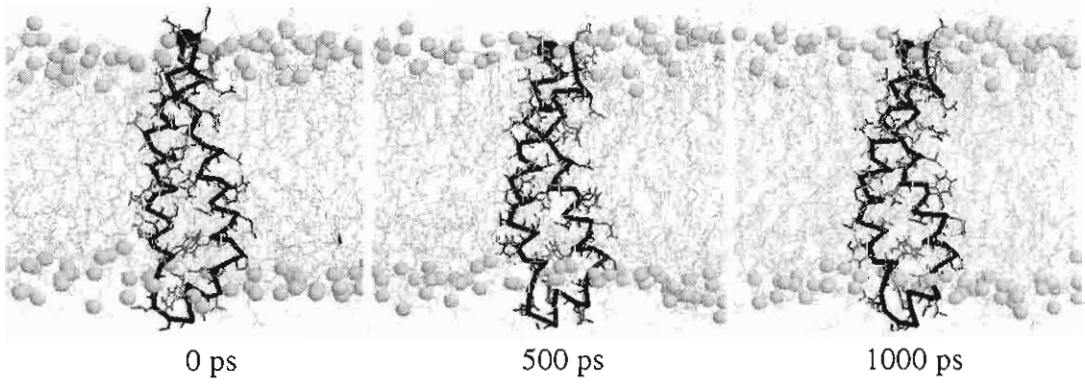

FIGURE 11 Snapshots of the Cry4B α4-α5 hairpin simulations in POPC bilayers. The water molecules on either side of the POPC bilayers are omitted for clarity. Backbone traces were shown as black rods while protein side-chains were indicated as gray stick. Gray spheres are marking positions of phosphate group of POPC molecules.

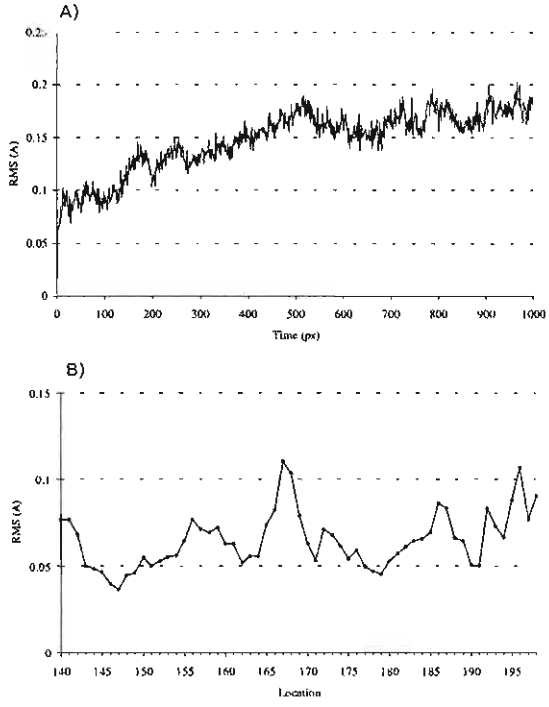

FIGURE 12 Root mean square deviation (A) and Root mean square fluctuation (B) of the α4-α5 helical hairpin during 1000 ps unrestrained molecular dynamics.

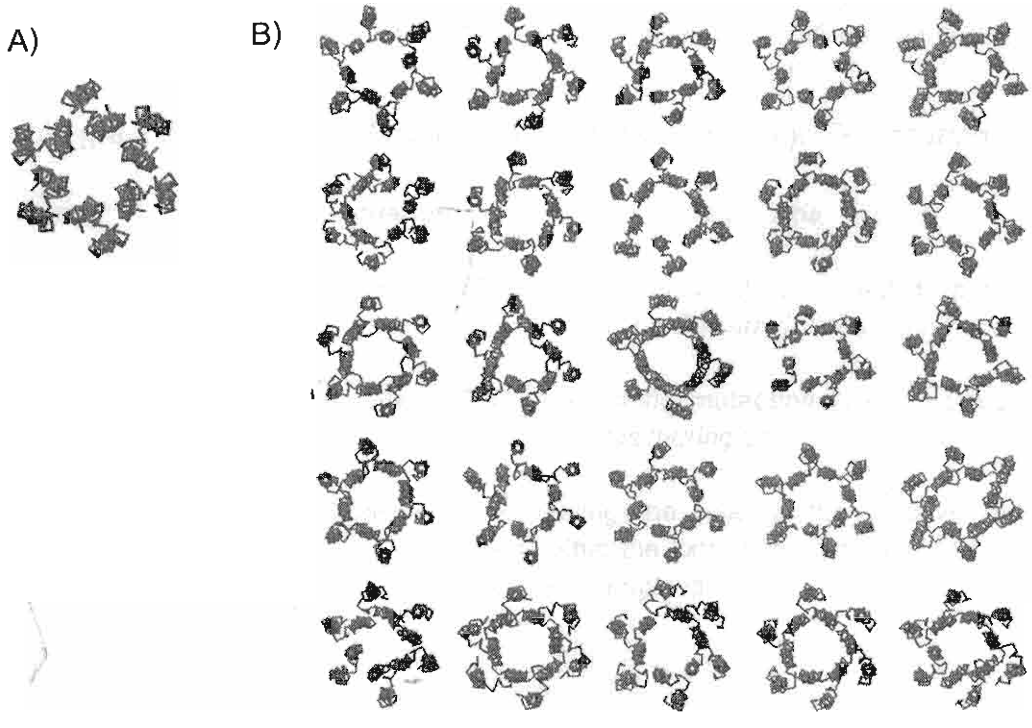

FIGURE 13 Models of initial structures of an oligomeric pore, consisting of 6 copies of α4-α5 hairpin before subjected to SA/MD (A) and 25 models which were generated after SA/MD (B).

Outputs

1. Publications:

1.1 Sramala, I., Uawithya, P., Chanama, U., Leetachewa, S., Krittanai, C., Katzenmeier, G., Panyim, S. and **Angsuthanasombat, C.** (2000) Single proline substitutions of selected helices of the *Bacillus thuringiensis* Cry4B toxin affect inclusion solubility and larvicidal activity. ***J. Biochem. Mol. Biol. Biophys.*** **4**:187-193.

1.2 Uawithya, P., Chanama, U., Potvin, L., Schwartz, J.L., Krittanai, C., Katzenmeier, G., Panyim, S. and **Angsuthanasombat, C.** (2000) Ion-channel formation in artificial lipid membranes by the *Bacillus thuringiensis* Cry4B toxin. ***Biophys. J.*** **78**:175A.

1.3 Sramala, I., Leetachewa, S., Krittanai, C., Katzenmeier, G., Panyim, S. and **Angsuthanasombat, C.** (2000) Charged residue Screening in helix 4 of the *Bacillus thuringiensis* Cry4B toxin reveals one critical residue for larvicidal activity. ***J. Biochem. Mol. Biol. Biophys.*** (in press).

1.4 Puntheeranurak, T., Leetachewa, S., Krittanai, C., Katzenmeier, G., Panyim, S. and **Angsuthanasombat, C.** (2000) Expression and Biochemical Characterisation of the *Bacillus thuringiensis* Cry4B α1-α5 pore forming fragment. ***J. Biochem.*** (in press).

2. Students graduated in **M.Sc.** (*Molecular Genetics and Genetic Engineering*):

Name	***Date of Graduation***	***Thesis Title***
Mr. Jongrak Kittiworakarn	Oct 26, 1998	Molecular studies of a putative pore-forming fragment of the *Bacillus thuringiensis* Cry4B toxin
Mr. Issala Sramara	May 28, 1999	Proline scanning mutagenesis of selected helices of the *Bacillus thuringiensis* Cry4B toxin
Ms. Walairat Pornwiroon	Jun 5, 2000	Investigating the role of the putative disulphide bond within the loop connecting α4 and α5 of the *Bacillus thuringiensis* toxin

.....

APPENDIX

Biochem. Mol. Biol. & Biophys., Vol. 4, pp. 187–193
Reprints available directly from the publisher
Photocopying permitted by license only

Single Proline Substitutions of Selected Helices of the *Bacillus thuringiensis* Cry4B Toxin Affect Inclusion Solubility and Larvicidal Activity

ISSARA SRAMALA[a], PANAPAT UAWITHYA[a], UMNAJ CHANAMA[b], SOMPHOB LEETACHEWA[a], CHARTCHAI KRITTANAI[a], GERD KATZENMEIER[a], SAKOL PANYIM[a] and CHANAN ANGSUTHANASOMBAT[a,*]

[a]*Institute of Molecular Biology and Genetics,* [b]*Central Equipment Laboratory, Institute of Science and Technology for Research and Development, Mahidol University, Salaya Campus, Nakornpathom, Thailand 73170*

(Received 8 November 1999; Revised 15 November 1999; Accepted 13 December 1999)

PCR-based mutagenesis was employed to investigate the role in toxicity of putative transmembrane helices of the 130-kDa Cry4B mosquito-larvicidal delta-endotoxin produced by *Bacillus thuringiensis* subsp. *israelensis*. Mutant toxins with a single proline substitution in the central region of α5, α6 and α7 were constructed and expressed in *Escherichia coli* as cytoplasmic inclusion bodies with a yield similar to that of the wild-type toxin. Unlike inclusions of the wild-type and that of the previous mutants for proline replacements in α3 or α4, all proline-substituted inclusions were insoluble in carbonate buffer, pH 9.0, indicating that the bend introduced in these three helices possibly interferes with the protein inclusion packing as shown by the insolubility. Similar to the previous substitution in α4, an almost complete loss of toxicity against *Aedes aegypti* mosquito-larvae was demonstrated for *E. coli* cells expressing mutant toxins in which residues Val-181, Ala-182 or Leu-186 in α5 were changed to proline. In addition, a dramatic decrease in larvicidal activity was observed for the substitution at Thr-254 in α7 while the mutation Q215P in α6 did not affect the biological activity. These results suggest that the central helix (α5) and conceivably α7, but not α6, are important determinants of toxin function. Our data therefore further support the notion that the putative pore forming helical hairpin α4–α5 together with α7 plays a crucial role in Cry toxin activity.

Keywords. *Bacillus thuringiensis*, Proline substitutions, Delta-endotoxins, Larvicidal activity, Inclusion solubility

INTRODUCTION

Bacillus thuringiensis (*Bt*) is a Gram-positive entomopathogenic bacterium that has been used successfully as an alternative insecticide for biological control of disease vectors and other pests. During sporulation, different *Bt* strains produce larvicidal proteins (classified as Cry and Cyt

* Corresponding author. Tel.: (662)-441-9003, ext. 1278. Fax: (662)-441-9906. E-mail: stcas@mahidol.ac.th.

lta-endotoxins) in large quantities as cytoplasmic ystalline inclusions that are specifically toxic to variety of dipteran, lepidopteran and coleopteran sect larvae [1,2]. When ingested by susceptible rvae, the inclusions are solubilised by the alkaline H of the larval midgut and the protoxins are tivated by gut proteases. It is believed that the tivated toxins then bind to midgut epithelial cells specific receptors, and insert into the microvillar embrane to form ion channels or leakage pores at cause cell swelling and eventually death by lloid-osmotic lysis (see [3] for reviews). However, e insecticidal mechanism at the molecular level of ese *Bt* toxins is still not entirely established.

The X-ray crystal structure of two different Cry xins, the coleopteran-specific Cry3A toxin [4] d the lepidopteran-specific Cry1Aa toxin [5], veals Cry proteins consisting of three distinct omains, and it is believed that each domain has defined function including pore formation and ceptor recognition [4,5]. Domain I is a group of ven α-helices in which the central helix (α5) is latively hydrophobic and encircled by six other mphipathic helices. Domain II is the most vari- ble part of the Cry toxin family and is composed three anti-parallel β-sheets, each terminating in surface-exposed loop. Domain III is a tightly acked β-sandwich of two anti-parallel sheets. has been proposed that other members of this mily will have the same overall tertiary structure nce the core of the molecule including all the omain interfaces is built up from five amino id sequence segments that are highly conserved roughout the entire Cry toxin family [1,4].

Structurally, it is immediately apparent that omain I is likely to be the transmembrane pore- rming apparatus. This domain contains five mphipathic helices (α3, α4, α5, α6 and α7) that e theoretically long enough to span the bilayer pid membrane and form a lytic pore [4,5]. The ssibility that this α-helical bundle in domain I essential for pore formation is supported by e feature that it is highly conserved in all Cry xins [1], and by analogy with the helical bundle pore-forming structures of two other well-characterised bacterial toxins, colicin A and diphtheria toxin, although they bear no sequence homology [6]. This notion is further supported by several studies with truncated proteins corresponding to domain I of Cry1Ac [7] and Cry3B2 [8] and with synthetic peptides of selected helices from Cry1Ac [9] or Cry3A [10] that demonstrated pore-forming activity either in phospholipid membrane vesicles or within planar lipid bilayers. A number of experiments via site-directed mutagenesis suggested that α4 and or α5 of Cry1Aa [11,12] and of Cry1Ac [13] and the loop between the bottoms of α4 and α5 of Cry1Ab [14] are involved in pore formation. Recently, we have employed single proline substitutions and demonstrated that α4, but not α3, of the dipteran-specific Cry4B toxin plays a crucial role in larvicidal activity, possibly in the pore-forming step rather than in receptor binding [15]. In this report, we have applied the same mutagenesis strategy to further investigate a possible involvement in toxicity of three other putative-transmembrane helices (α5, α6 and α7) of this mosquito-active toxin, and found that these three helices are essentially involved in inclusion solubility. Our results also indicate that α5 and α7, but not α6, play a role in larvicidal activity of the Cry4B toxin.

MATERIALS AND METHODS

Construction and Expression of Mutant Toxins

Single proline substitutions via *in vitro* site-directed mutagenesis were performed using a Quickchange PCR-based mutagenesis kit (Stratagene) following the manufacturer's instructions. The plasmid pMU388, constructed by cloning the full-length *cry4B* toxin gene from *Bt* subsp. *israelensis* in a pUC12 vector [16], was used as a template. Mutagenic primers were purchased from Bio-synthesis Inc. (USA) as shown in Table I. All mutations were verified by DNA sequencing using an ABI prism 377 sequencer.

TABLE 1 Oligonucleotide primers designed to substitute a coded residue with proline

Primer	Location	Sequence[a]	Restriction site
	α5	P I Y A Q **P** A N F N L	
V181P-f		CCAATATACGCACAA<u>CCGG</u>CAAATTTCAATTTAC	*Hpa*II
V181P-r		GTAAATTGAAATTTG<u>CCGG</u>TTGTGCGTATATTGG	
	α5	P I Y A Q V **P** N F N L	
A182P-f		CCAATATACGCACA<u>GGTCC</u>CAAATTTCAATTTAC	*Sau*96I
A182P-r		GTAAATTGAAATTTG<u>GGAC</u>CTGTGCGTATATTGG	
	α5	A N F N **P** L L I R D G L	
L186P-f		GCAAATTTCAATCCACTTTTAAT<u>CCGG</u>GATGGCCTC	*Hpa*II
L186P-r		GAGGCCATC<u>CCGG</u>ATTAAAAGTGGATTGAAATTTGC	
	α6	T M V **P** Y T K E Y I	
Q215P-f		CACTATGGTGC<u>CGTATAC</u>TAAAGAATATATTGC	*Acc*I
Q215P-r		GCAATATATTCTTTA<u>GTATAC</u>GGCACCATAGTG	
	α7	D T K R E M **P** I Q V L	
T254P-f		GATTATAAAAGAGAGATGCC<u>GATTC</u>AAGTATTAG	*Hmf*I
T254P-r		CTAATACTT<u>GAATC</u>GGCATCTCTCTTTTATAATC	

[a]Introduced restriction enzyme recognition sites are underlined. Mutated nucleotide residues are shown as boldface. The deduced amino acid sequence is shown above each oligonucleotide sequence.

Partial Purification and Solubilisation of Protoxin Inclusions

The wild type and mutant Cry4B toxin genes were expressed in *E. coli* strain JM109 under control of the *lac*Z promoter. Cells were grown in LB medium plus 100 μg/ml of ampicillin until OD_{600} reached 0.4–0.5 and incubation was continued for another 4 h after addition of isopropyl-β-D-thiogalacto pyranoside (IPTG) to a final concentration of 0.1 mM. *E. coli* cultures expressing each mutant as inclusion bodies were harvested by centrifugation, resuspended in 1 ml of distilled water and then disrupted in a French Pressure Cell at 16,000 psi. The crude lysates were centrifuged at 8000*g* for 5 min and pellets obtained were washed 3 times in distilled water. Protein concentrations were determined by using a protein microassay (Bio-Rad), with bovine serum albumin fraction V (Sigma) as a standard.

Protoxin inclusions (1 mg/ml) were solubilised in 50 mM Na_2CO_3, pH 9.0 and incubated at 37°C for 60 min as described previously [15]. After centrifugation for 10 min, the supernatants were analysed by SDS-15% (w/v) polyacrylamide gel electrophoresis (PAGE) in comparison with the inclusion suspension.

Larvicidal Activity Assays

Bioassays were performed as described previ ously [15] with some modification using 2-day-ol *Aedes aegypti* mosquito-larvae reared in a containe (22 × 30 × 10 cm deep) with approximately 31 o distilled water supplemented with a small amoun of rat diet pellets. Both rearing and bioassays wer done at room temperature (25°C). The assays wer carried out in 1 ml of *E. coli* suspension (10^8 cell suspended in distilled water) in a 48-well microtitr plate (11.3 mm well diameter), with 10 larvae pe well and a total of 100 larvae for each type c *E.coli* samples. Mortality was recorded after 24- incubation period.

RESULTS AND DISCUSSION

Recently, data on molecular determinants of men brane insertion and pore formation for *Bt* Cr toxins has increased substantially. Where studie the helical domain of different Cry toxins has no been putatively demonstrated to be involved i membrane integration and toxin pore formatic [7–15]. In the present study, we have made use

PCR-based mutagenesis to construct several more mutants in the putative pore-forming domain to determine which of the three other helices (α5, α6 or α7) would be responsible for toxicity of the mosquito-active Cry4B toxin. Proline substituted mutants were designed based on a 3D Cry4B model which was previously constructed by homology modelling using Cry3A as a template [17]. The designed mutants have single proline substitutions in the central region of the selected helices of Cry4B including α5 at residues Val-181, Ala-182 and Leu-186, α6 at Gln-215 and α7 at Thr-254 (Fig. 1). Each mutant gene could be over-expressed in *E. coli* under inducible control of the *lac*Z

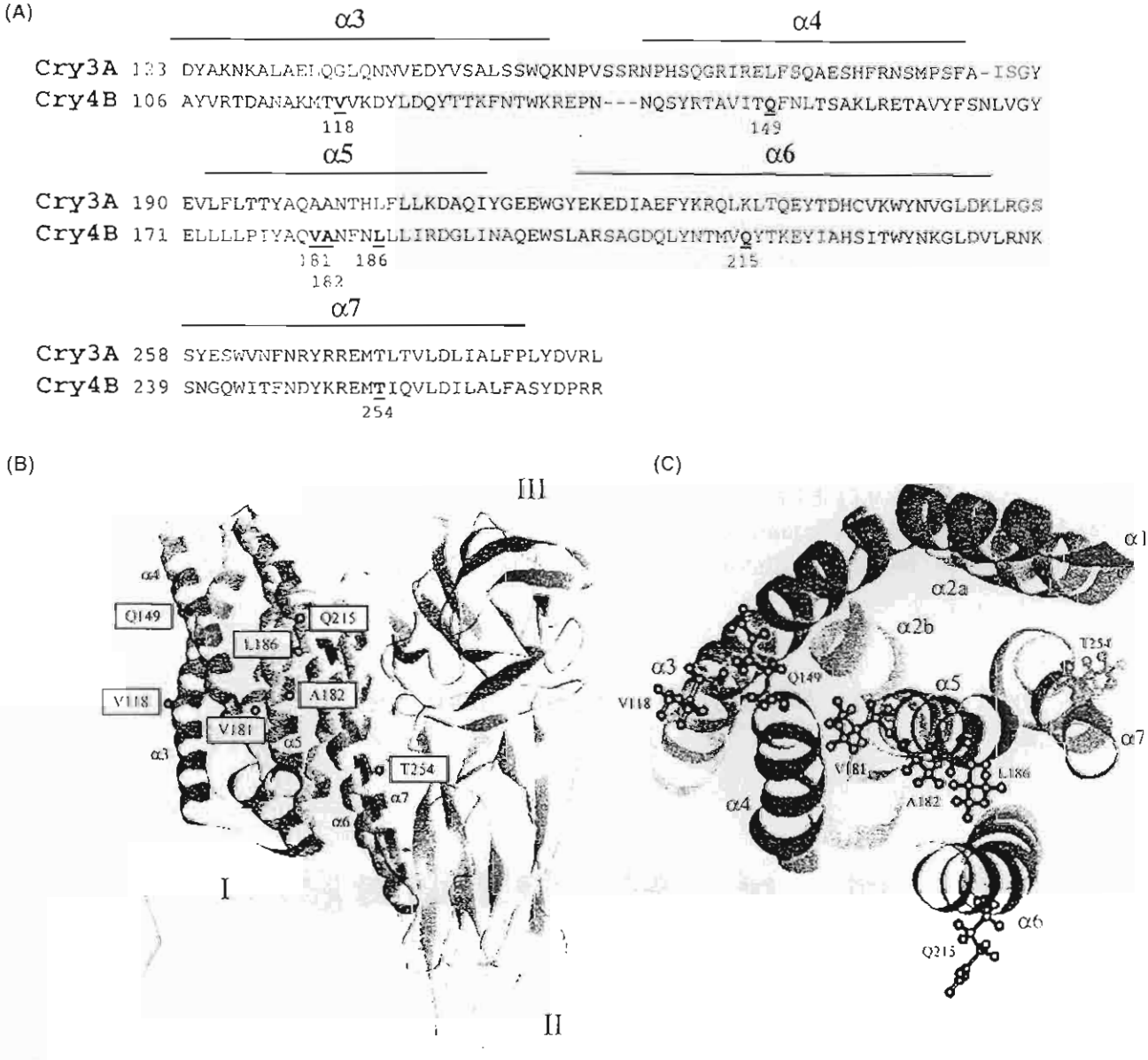

FIGURE 1 (A) Amino acid sequence alignment of Cry4B with the known secondary structure elements of Cry3A. Single proline substitutions at each indicated position are underlined and emboldened. The corresponding helices are shown above the sequences. (B) A ribbon representation (generated by Weblab viewer, Molecular Simulation Inc.) of the Cry4B model built by homology modelling [17], illustrating the three-domain organisation (I–III). Black beads indicate β-carbon atoms of the mutated residues. (C) Top view of the helical bundle in domain I of Cry4B. The mutated residues are shown as ball and stick: α3 at Val-118, α4 at Gln-149, α5 at Val-181, Ala-182, and Leu-186, α6 at Gln-215 and α7 at Thr-254.

romoter by addition of IPTG to mid-exponential hase cultures and the mutant toxins were preominantly produced as sedimentable inclusion odies which were then partially purified. In addi-ion, the level of protein expression of all mutant roteins was approximately the same as that of he wild type, and the expressed mutant derivatives till cross-reacted with Cry4B antibodies (data not hown).

Experiments were carried out to assess the solu-ility of mutant protein inclusions in carbonate uffer, pH 9.0 in comparison with that of the wild-ype inclusion. The amounts of the 130-kDa solu-le proteins in the supernatant were compared vith those of the proteins initially used in order to etermine the percentage of protein solubilisation. A complete loss of solubility at alkaline pH was bserved for the inclusions of the mutants sub-tituted in $\alpha5$, $\alpha6$ or $\alpha7$, whilst the inclusions of he two previously constructed mutants, V118P nd Q149P, exhibited the same solubility charac-eristics as that of the wild-type (Fig. 2). The reason or the difference in solubility between those two ets of point mutations is not clear. However, this nay be explained by the fact that all the five nutated residues, i.e. Val-181, Ala-182 and Leu-186 in $\alpha5$, Gln-215 in $\alpha6$ and Thr-254 in $\alpha7$ are buried in the protein core, unlike Val-118 in $\alpha3$ and Gln-149 in $\alpha4$ that are exposed at the protein surface (see Fig. 1C). Thus, the bend created by the proline substitution in these relatively conserved helices, i.e. $\alpha5$, $\alpha6$ or $\alpha7$ possibly disturbs the structural characteristics either locally or globally that might consequently affect inclusion formation as demonstrated by a drastically perturbed dissolvability. On the other hand, the proline mutations in $\alpha3$ or $\alpha4$ appear to affect only the individual helices, without significantly influencing the other helices or the overall structure, as earlier demonstrated for an α-lactalbumin folding intermediate [18].

To determine whether a single proline replacement in these three additional helices also affects the larvicidal activity of Cry4B, *E. coli* cells expressing each type of the mutant toxins were bioassayed using *Aedes aegypti* mosquito-larvae (Fig. 3). The mortality data recorded after a 24-h incubation reveals that the $\alpha6$ mutant (Q215P) still exhibited full larvicidal activity ($98.7 \pm 0.7\%$) similar to the $\alpha3$ mutant (V118P), whereas the T254P mutant produced merely $23.7 \pm 13.9\%$. However, mortality of all the $\alpha5$ mutants, V181P, A182P and L186P, was almost totally abolished as approximately

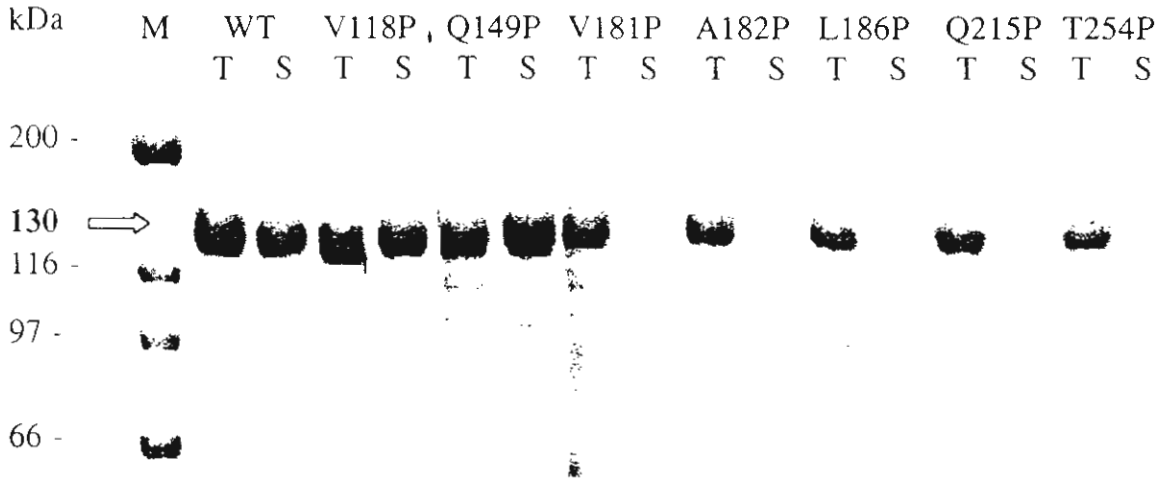

FIGURE 2 The figure shows a Coomasie brilliant blue-stained SDS-15% polyacrylamide gel of the partially purified 130-kDa protein inclusions extracted from *E. coli* expressing the wild-type (WT) and mutant Cry4B toxins and solubilised in carbonate buffer. (T) and (S) represent the total fractions and an equivalent volume of the supernatants after centrifugation, respectively. (M) represents the molecular mass standards.

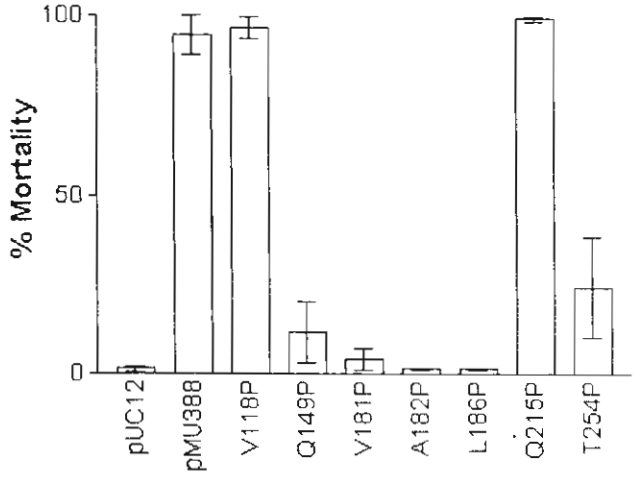

FIGURE 3 Larvicidal activities of *E. coli* cells expressing either the Cry4B wild-type toxin (pMU388) and its mutants (V118P, Q149P, V181P, A182P, L186P, Q215P and T254P) against *A. aegypti* larvae. Error bars indicate standard error of the mean from three independent experiments.

comparable to that observed with the previously described $\alpha4$ mutant (Q149P). These results suggest that the integrity of $\alpha5$ and $\alpha7$ may indeed be important for toxin activity like that of $\alpha4$.

Although toxin inclusion insolubility and larvicidal activity are seemingly correlated for all the three $\alpha5$ mutants and the $\alpha7$ mutant, the insolubility *in vitro* may not always necessarily reflect toxin activity *in vivo* as observed for the $\alpha6$ mutant which was insoluble at pH 9.0 but still bioactive. It has been previously demonstrated that the difference detected in solubilisation *in vitro* for Cry4A inclusions which were purified from two different *Bt* recipient strains, is not a factor in larval toxicity [19]. Presumably, larval midgut proteases *in vivo* might facilitate the dissolution of the ingested toxin inclusions which would negate the differences between the observed toxicities of the $\alpha3$ and $\alpha6$ mutants. It was shown that incubation of the Cry2A toxin with gut proteases enhanced the solubility of the toxin inclusion, obviating the requirement for reducing agents at pH 10.5 [20].

In conclusion, this report additionally demonstrates that the central helix ($\alpha5$), $\alpha6$ and $\alpha7$, but not $\alpha3$ or $\alpha4$, are conceivably involved in protein packing for inclusion formation, thus destabilising these three helices individually could give rise to toxin insolubility *in vitro*. Moreover, our study also provides further support for a crucial role of the pore-forming helical hairpin $\alpha4$–$\alpha5$ as well as $\alpha7$, which has been suggested to be a domain binding sensor [10], in larvicidal activity of the Cry4B toxin.

Acknowledgements

We thank Miss. Chanikarn Boonchuoy for her excellent technical support with DNA sequencing. Mrs. Anchalee Nirachanon and Miss. Shaweewan Shimwai for technical assistance. We are also grateful to Dr. Albert J. Ketterman for his helpful comments and discussion. This work was supported by the National Science and Technology Development Agency and the Thailand Research Fund.

References

[1] Hofte, H. and Whiteley, H.R. Insecticidal crystal proteins of *Bacillus thuringiensis*. *Microbiol. Rev.* 1989; **53**: 242–255.
[2] Schnepf, E., Crickmore, N., Van Rie, J., Lereclus, D., Baum, J., Feitelson, J., Zeigler, D.R. and Dean, D.H. Microbiology *Bacillus thuringiensis* and its pesticidal crystal proteins. *Mol. Biol. Rev.* 1998; **62**: 775–806.
[3] Knowles, B.H. Mechanism of action of *Bacillus thuringiensis* insecticidal δ-endotoxins. *Adv. Insect Physiol.* 1994; **24**: 275–308.
[4] Li, J., Carroll, J. and Ellar, D.J. Crystal structure of insecticidal delta-endotoxin *from Bacillus thuringiensis* at 2.5 A resolution. *Nature* 1991; **353**: 815–821.
[5] Grochulski, P., Masson, L., Borisova, S., Pusztai-Carey, M., Schwartz, J.L., Brousseau, R. and Cygler, M. *Bacillus thuringiensis* CryIA(a) insecticidal toxin: crystal structure and channel formation. *J. Mol. Biol.* 1995; **254**: 447–464.
[6] Parker, M.W. and Pattus, F. Rendering a membrane protein soluble in water: a common packing motif in bacterial protein toxins. *Trends Biochem. Sci.* 1993; **18**: 391–395.
[7] Walters, F.S., Slatin, S.L., Kulesza, C.A. and English, L.H. Ion channel activity of N-terminal fragments from CryIA(c) delta-endotoxin. *Biochem. Biophys. Res. Commun.* 1993; **196**: 921–926.
[8] Von Tersch, M.A., Slatin, S.L., Kulesza, C.A. and English, L.H. Membrane-permeabilizing activities of *Bacillus thuringiensis* coleopteran-active toxin CryIIIB2 and CryIIIB2 domain I peptide. *Appl. Environ. Microbiol.* 1994; **60**: 3711–3717.
[9] Cummings, C.E. and Ellar, D.J. Structural and functional studies of a synthetic peptide mimicking a proposed membrane inserting region of a *Bacillus thuringiensis* delta-endotoxin. *Microbiology* 1994; **140**: 2737–2747.
[10] Gazit, E., La Rocca, P., Sansom, M.S.P. and Shai, Y. The structure and organization within the membrane of the helices composing the pore-forming domain of *Bacillus thuringiensis* delta-endotoxin are consistent with an

"umbrella-like" structure of the pore. *Proc. Natl. Acad. Sci. USA* 1998; **95**: 12 289–12 294.

[11] Schwartz, J.L., Juteau, M., Grochulski, P., Cygler, M., Prefontaine, G., Brousseau, R. and Masson, L. Restriction of intramolecular movements within the Cry1Aa toxin molecule of *Bacillus thuringiensis* through disulfide bond engineering. *FEBS Lett.* 1997; **410**: 397–402.

[12] Ahmad, W. and Ellar, D.J. Directed mutagenesis of selected regions of a *Bacillus thuringiensis* entomocidal protein. *FEMS Microbiol. Lett.* 1990; **56**: 97–104.

[13] Kumar, A.S. and Aronson, A.I. Analysis of mutations in the pore-forming region essential for insecticidal activity of a *Bacillus thuringiensis* delta-endotoxin. *J. Bacteriol.* 1999; **181**: 6103–6107.

[14] Chen, X.J., Curtiss, A., Alcantara, E. and Dean, D.H. Mutations in domain 1 of *Bacillus thuringiensis* delta-endotoxin Cry1Ab reduce the irreversible binding of toxin to *Manduca sexta* brush border membrane vesicles. *J. Biol. Chem.* 1995; **270**: 6412–6419.

[15] Uawithya, P., Tuntitippawan, T., Katzenmeier, G., Panyim, S. and Angsuthanasombat, C. Effects on larvicidal activity of single proline substitutions in α3 or α4 of the *Bacillus thuringiensis* Cry4B toxin. *Mol. Biol. Inter.* 1998; **44**: 825–832.

[16] Angsuthanasombat, C., Chungjatupornchai, W., Kertbundit, S., Luxananil, P., Settasatian, C., Wilairat, P. and Panyim, S. Cloning and expression of 130-kd mosquito-larvicidal delta-endotoxin gene of *Bacillus thuringiensis* var. *israelensis* in *Escherichia coli*. *Mol. Gen. Genet.* 1987; **208**: 384–389.

[17] Uawithya, P., Krittanai, C., Katzenmeier, G., Leetachewa, S., Panyim, S. and Angsuthanasombat, C. 3D models for *Bacillus thuringiensis* Cry4A and Cry4B insecticidal proteins based on homology modelling. Abstract 32nd Meeting, Society for Invertebrate Pathology, Irvine, USA, 1999; p. 75.

[18] Schulman, B.A. and Kim, P.S. Proline scanning mutagenesis of a molten globule reveals non-cooperative formation of a protein's overall topology. *Nat. Struct. Biol.* 1996; **3**(8): 682–687

[19] Angsuthanasombat, C., Crickmore, N. and Ellar, D.J. Comparison of *Bacillus thuringiensis* subsp. *israelensis* CryIVA and CryIVB cloned toxins reveals synergism *in vivo*. *FEMS Microbiol. Lett.* 1992; **94**: 63–68.

[20] Nicholls, C.N., Ahmad, W. and Ellar, D.J. Evidence for two different types of insecticidal P2 toxins with dual specificity in *Bacillus thuringiensis* subspecies. *J. Bacteriol.* 1989; **171**: 5141–5147.

J. Biochem. Mol. Biol. & Biophys., Vol. ..., pp. 1-7
Reprints available directly from the publisher
Photocopying permitted by license only

Charged Residue Screening in Helix 4 of the *Bacillus thuringiensis* Cry4B Toxin Reveals One Critical Residue for Larvicidal Activity

ISSARA SRAMALA, SOMPHOB LEETACHEEWA, CHARTCHAI KRITTANAI, GERD KATZENMEIER, SAKOL PANYIM AND CHANAN ANGSUTHANASOMBAT*

Laboratory of Molecular Biophysics, Institute of Molecular Biology and Genetics, Mahidol University, Salaya Campus, Nakornpathom, Thailand 73170

(Receive 27 July 2000; Accepted 14 August 2000)

The different Cry δ-endotoxins produced by *Bacillus thuringiensis* have been shown to kill susceptible insect larvae by forming a lytic pore in the target midgut epithelial cell membrane. We have previously employed single proline substitutions *via* PCR-based mutagenesis and demonstrated that helices 4 and 5 in the pore-forming domain of the 130-kDa Cry4B toxin are essential for mosquito-larvicidal activity against *Aedes aegypti*. To further identify critical residues for toxicity, substitutions with alanine of each of the charged amino acids (Arg-143, Lys-156, Arg-158 and Glu-159) and one polar residue (Asn-151) in the transmembrane helix 4 were performed. Similar to the wild-type Cry4B protoxin, all five mutant toxins were over-expressed as cytoplasmic inclusions in *Escherichia coli* and were structurally stable upon solubilisation and trypsin activation in carbonate buffer, pH 9.0. Interestingly, a complete loss of activity against *A. aegypti* larvae was observed for the alanine substitution at Arg-158, while replacements at the four other positions did not affect the toxicity. The results reveal a crucial role in toxin function for the positively charged side chain of Arg-158 in helix 4 of the Cry4B toxin.

Keywords: *Bacillus thuringiensis*, Charged-to-alanine mutagenesis, Delta-endotoxins, Larvicidal activity

INTRODUCTION

Subspecies of the Gram-positive bacterium *Bacillus thuringiensis* (*Bt*) produce insecticidal proteins as different forms of parasporal crystalline inclusions during sporulation [1]. These cytoplasmic inclusions are composed of one or several polypeptides that have been classified as Cry and/or Cyt δ-endotoxins according to the similarity of their deduced amino acid sequences [2,3]. To date, the Cry toxins have been shown to be active

* Corresponding author. Tel: (662)-441-9003 ext. 1278; Fax: (662)-441-9906; stcas@mahidol.ac.th

against the larvae of major insect crop pests and disease vectors [4]. For instance, the 130-kDa Cry4B toxin from *Bt* subsp. *israelensis* is specifically toxic to mosquito larvae [2,4].

In the *Bt* inclusion bodies, the δ-endotoxins exist as inactive protoxins which require solubilisation and proteolytic activation in the insect larval midgut [1]. It has been proposed that after activation, the active toxins form pores *via* a two-step receptor mediated mechanism, in which the initial toxin-receptor interaction is followed by membrane insertion of the toxins to form transmembrane leakage pores. These pores cause the midgut epithelial cells to swell and lyse by colloid-osmotic lysis [5], resulting in extensive damage to the midgut and eventually larval death (see [6] for reviews). However, the molecular mechanism of the *Bt* toxins is still not entirely understood, although knowledge of how these insecticidal proteins function has increased substantially over the last decade.

Currently, the crystal structures of two different Cry toxins, Cry1Aa and Cry3A, have been determined by X-ray crystallography [7,8]. Both structures display a high degree of overall structural similarity and are composed of three structurally distinct domains [7,8]. It is apparent that the N-terminal domain, a seven-helix bundle, is clearly equipped for pore formation in the membrane [8]. This suggestion has been supported by studies that demonstrated that this helical domain is indeed responsible for pore-forming activity [9,10]. For the mechanism of membrane insertion and pore formation of the Cry toxins, an umbrella model seems to best explain the molecular mechanism [6]. In this model, helices 4 and 5 form a helical hairpin to initiate membrane penetration. After insertion of this hairpin, the other helices spread over the membrane surface followed by oligomerisation of the toxin [11,12], resulting in formation of an initial tetrameric pore [13]. This umbrella model is now noticeably supported by a number of experiments demonstrating a crucial role of α4 and α5 in pore-forming activity [14,15]. In addition, recent studies have demonstrated tha the α4-loop-α5 hairpin is more active in membrane penetration than each of the isolatec helices or their mixtures, supporting its functior as the membrane-inserted portion of the Cry toxins [16].

In the previous studies, we have employed single proline substitutions and demonstrated that α4 and α5 of the Cry4B toxin are important determinants of larvicidal activity, likely to be involved in pore formation rather than in receptor binding [17,18]. As an extension of the earlier studies, attempts have been made to investigate a possible involvement in toxicity of charged-residues in the helix 4 and found that elimination of the charged side chain at Arg-158 considerably affected larvicidal activity. Our results further support the important role of α4 in Cry toxin function.

MATERIALS AND METHODS

Site-Directed Mutagenesis

The plasmid pMU388 containing the full-length *cry4B* toxin gene from *Bt* subsp. *israelensis* in the pUC12 vector [19] was used as a template for site-directed mutagenesis. Complementary mutagenic oligonucleotides were purchased from Genset Inc. (Singapore) as shown in Table I. All mutations were performed using a Quickchange PCR-based mutagenesis kit (Stratagene) following the manufacturer's instructions. All mutants were analysed by DNA sequencing using a Perkin Elmer ABI prism 377 automated sequencer.

Toxin Expression and Preparation

All protoxins were produced as inclusion bodies in *E. coli* strain JM109 under inducible control of the *lacZ* promoter by addition of isopropyl-β-D-thiogalactopyranoside (IPTG), and partially purified as described earlier [17].

Protein concentrations were determined using a protein microassay (Bio-Rad) with BSA as a standard. The solubilised protoxins were assessed for their proteolytic stability by digestion with trypsin (L-1-tosylamide-2-phenylethyl chloromethyl ketone treated, Sigma) at a protoxin:trypsin ratio of 20:1 (w/w) for 16 hours [20]. All samples were analyzed by sodium dodecyl sulfate (SDS)-15% w/v polyacrylamide gel electrophoresis (PAGE).

Mosquito-Larvicidal Assays

Larvicidal activity assays were performed as previously described [18] using 2-day old *Aedes aegypti* larvae reared from eggs supplied by the mosquito-rearing facility of the Institute of Molecular Biology and Genetics, Mahidol University, Thailand. About 500 larvae were reared in a container (22×30×10 cm deep) with approximately 3 l of distilled water supplemented with 0.2-0.3 g of rat diet pellets. In the assays, 1 ml of *E. coli* suspension (ca. 10^8 cells) was added to a 48-well microtitre plate (11.3 mm well diameter), with 10 larvae per well and a total of 100 larvae for each type of *E. coli* sample. *E. coli* cells containing the recombinant plasmid pMU388 and the pUC12 vector were used as positive and negative controls, respectively. Mortality was recorded after incubation for 24 hours.

TABLE I Complementary mutagenic oligonucleotides for substituting a coded residue with alanine

Primer	Sequence[a]	Restriction Site
	Q S Y **A** T A V I T	
R143A-f	CCAGTCCTAT**GC**AACAGC**T**GTAATAACTC	*Pvu*II
R143A-r	GAGTTATTAC**A**GCTGTT**GC**ATAGGACTGG	
	V I T Q F **A** L T S A	
N151A-f	GTAATAACTCAATTT**GC**GTTAACCAGTGCC	*Hinc*II
N151A-r	GGCACTGGTTAA**CGC**AAATTGAGTTATTAC	
	L T S A **A** L R E T A	
K156A-f	CTTAACCAGTGCC**GC**ACTCCGGGAGACCGCAG	*Hpa*II
K156A-r	CTGCGGTCTCCCGGAGT**GC**GGCACTGGTTAAG	
	T S A K L **A** E T A	
R158A-f	CCAGTGCCAAGCTT**GC**AGAGACCGCAG	*Hind*III
R158A-r	CTGCGGTCTCT**GC**AAGCTTGGCACTGG	
	A K L R **A** T A V Y F S	
E159A-f	GCCAAACTTCGAG**C**GAC**T**GCAGTTTATTTTAGC	*Pst*I
E159A-r	GCTAAAATAAACTGC**A**GTC**G**CTCGAAGTTTGGC	

[a]Introduced restriction enzyme recognition sites are underlined. The mutated nucleotide residues are showed as boldface. Deduced amino acid sequences are shown on top of each pair of oligonucleotide primers.

RESULTS AND DISCUSSION

As predicted from the homology-based model of Cry4B [21], helix 4 is composed of 26 amino acids of which four are charged (see Fig. 1A). These charged residues, Arg-143, Lys-156, Arg-158 and Glu-159, are widely distributed along the hydrophilic surface (Fig. 1B). In the present study, five Cry4B mutants, R143A, N151A, K156A, R158A and E159A, were generated at five different positions (see Fig. 1C) by substituting each relevant residue with alanine *via* PCR-based mutagenesis. The energy-minimised models for these mutants suggested

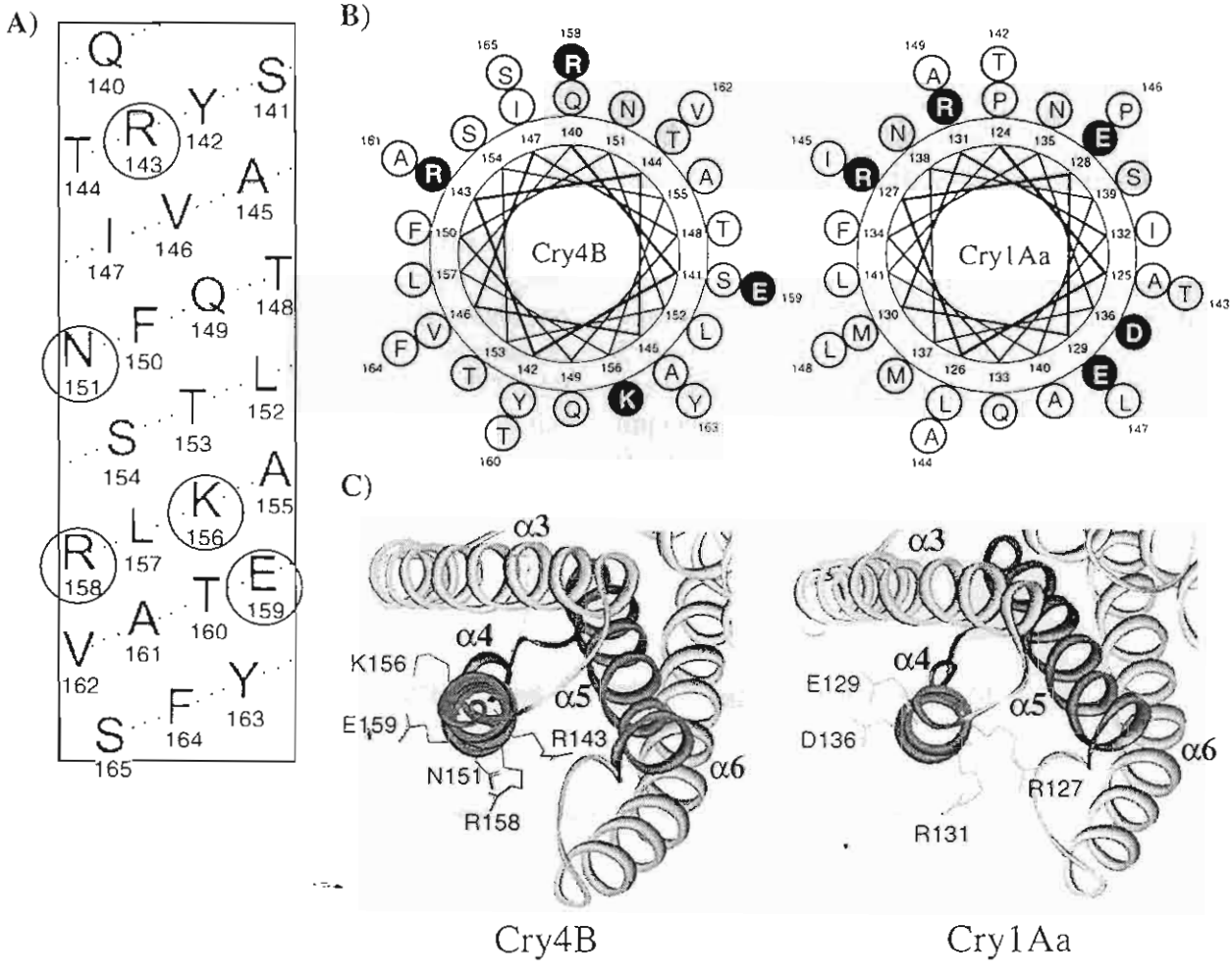

FIGURE 1 (A): A predicted pattern of helix 4 of Cry4B redrawn from [20] is composed of 26 residues of which the encircled residues were substituted by alanine. (B): Helical wheel projections of helix 4 of Cry4B and Cry1Aa. Amino acid residues are plotted every 100 degrees consecutive around the wheel, following the sequences given in A and [15] for Cry4B and Cry1Aa, respectively. The following colour code is used: black is an amino acid with a charged side chain; gray is a polar side chain and white is a hydrophobic side chain. (C): Top views of amino acid arrangement in helix 4 together with the relative positions of helices 3, 5 and 6 in a 3D Cry4B model built by homology modelling [21] and the Cry1Aa structure [7]. The labeled residues indicate the targeted positions. The structures were prepared using Weblab viewer (Molecular Simulation Inc.).

that each point mutation would not cause drastic changes in the overall structure of the mutant toxins.

Upon induction with IPTG, *E. coli* cells transformed with each mutant plasmid highly expressed the 130-kDa Cry4B derivatives as inclusion bodies with a yield comparable to the wild-type toxin. After partial purification, protein preparations were analysed by SDS-PAGE and all shown to contain more than 90% pure Cry proteins (Fig. 2, lanes 2,4,6,8, 10 and 12). In addition, all mutant protein inclusions were found to be soluble in carbonate buffer, pH 9.0, giving at least 70% solubility which resembles closely the wild-type inclusions under similar conditions [17]. The solubilised mutant protoxins were also examined for their proteolytic stability by digestion with trypsin and all found to produce protease-resistant products of ca. 47 and ca. 21 kDa identical to the wild-type protoxin (Fig. 2, lanes 3,5,7,9,11 and 13) [20]. These results suggested that all the mutant protoxins containing alanine substitutions had folded to their native conformation.

E. coli cells expressing each type of the mutant toxin were tested for their relative toxicity against *Aedes aegypti*. All assays were carried out in ten replicas for each sample and repeated three times; the mortality data recorded after a 24-hour incubation are shown in Fig. 3. Compared with wild-type Cry4B, four mutants with alanine substitutions at charged residues (Arg-143, Lys-156 and Glu-159) or at one polar residue (Asn-151) exhibited no loss of larvicidal activity. In contrast, one mutant with the alteration of a charged amino acid at Arg-158 was not active against the larvae.

As suggested by solubilisation and trypsin activation of the Cry4B protoxin, the mutations did not induce structural distortions in the toxin molecule. Therefore, the complete loss of toxicity observed for the R158A mutant is least likely to be caused by misfolding of the protein. Considered as a whole, our results indicate that the side of helix 4 containing Arg-158 is an important determinant for larvicidal activity of the Cry4B toxin. This notion is supported by experimental results obtained with directed

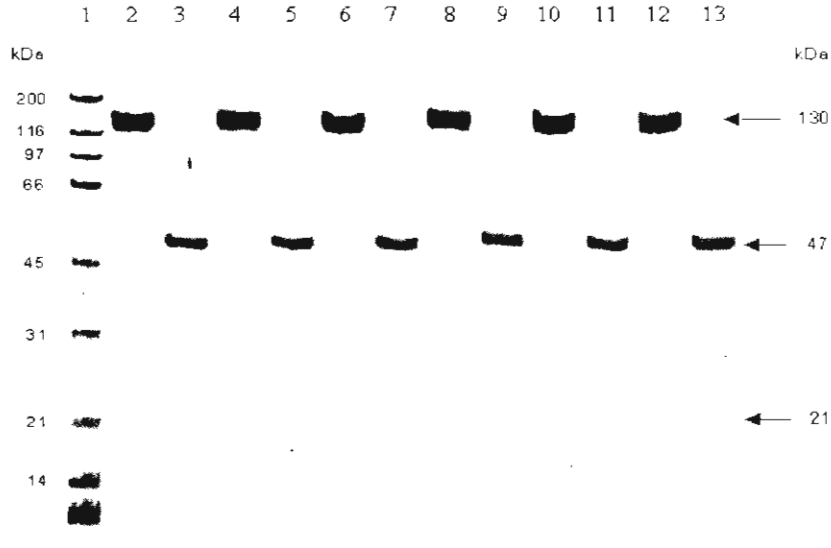

FIGURE 2 Coomassie brilliant blue-stained SDS-15% polyacrylamide gel comparing the yields of solubilised protoxins and their trypsin-cleavage products. Lane 1 represents molecular mass standards. Lanes 2, 4, 6, 8, 10 and 12 are the solubilised 130-kDa Cry4B protein and its mutant protoxins R143A, N151A, K156A, R158A and E159A, respectively. Lanes 3, 5, 7, 9, 11 and 13 are trypsin-cleavage products of the above samples run in the same order.

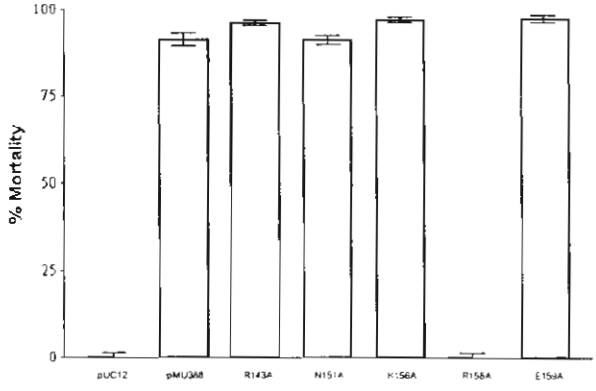

FIGURE 3 Mosquito-larvicidal activities of *E. coli* cells expressing the Cry4B wild-type toxin (pMU388) or its mutants (R143A, N151A, K156A, R158A and E159A) against *Aedes aegypti* larvae. Error bars indicate standard error of the mean from three independent experiments.

substitutions of helix 4 residues in other Cry proteins, Cry1Aa and Cry1Ac [14,15].

Recently, Masson *et al.* [15] have constructed a series of charged residue mutants in helix 4 of the Cry1Aa toxin. The mutant toxins were tested for toxicity against *Plutella xylostella* diamondback moth larvae and found that mutants with alterations at Glu-129, Arg-131 or Asp-136 showed a complete loss of larvicidal activity. Based on conductance experiments with planar lipid bilayers, the authors have concluded that loss of toxicity was caused by prevention of formation of ion channels in these mutants and that the negative charge of Asp-136 and Glu-129 contributes directly to the passage of ions through the transmembrane pore. Interestingly, their positively charged non-toxic mutant R131Q displayed reduced conductance, albeit the structural basis for this observation is not clear yet. For the Cry1Ac toxin, the R131L substitution has been shown to cause a 10-fold reduction in toxicity against *Manduca sexta* tobacco hornworm [14]. We have recently constructed a homology model for the Cry4B toxin [21] in which Arg-158 is located on the same side of helix 4 relative to Arg-131 in the Cry1Aa toxin [7] (see Fig. 1B&C). Despite a relatively high degree of similarity in both structures, our experiment revealed that elimination of the only negatively charged side chain in helix 4, Glu-159, which corresponds to Asp-136 in Cry1Aa (Fig. 1C), did not affect toxin activity of Cry4B. It is conceivable that these differences in response to modification of charged residues reflect subclass-specific variations in the channel architecture for individual Cry proteins. Further experimentation is required to answer the question whether alanine substitutions at Arg-158 and Glu-159 are conducive to alterations in the passage of ions through the pore.

Acknowledgements

We are grateful to Prof. Prapon Wilairat and Dr. Albert Ketterman for valuable comments. We also thank C. Boonchuoy for excellent technical support with DNA sequencing; U. Chanama, A. Nirachanon and S. Shimwai for technical assistance. This work was supported in part by the National Science and Technology Development Agency and the Thailand Research Fund. A Royal Golden Jubilee Ph.D. research scholarship to I.S. is gratefully acknowledged.

References

[1] Aronson, A.I., Beckman, W. and Dunn, P. *Bacillus thuringiensis* and related insect pathogens. *Microbiol. Rev.* 1986; **50**: 1-24.

[2] Hofte, H. and Whiteley H.R. Insecticidal crystal proteins of *Bacillus thuringiensis*. *Microbiol. Rev.* 1989; **53**: 242-255.

[3] Crickmore, N., Zeigler, D.R., Feitelson, I., Schnepf, E., Van Rie, J., Lereclus, D., Baum, J. and Dean, D.H. Revision of the nomenclature for the *Bacillus thuringiensis* pesticidal crystal proteins. *Microbiol. Mol. Biol. Rev.* 1998; **62**: 807-813.

[4] Schnepf, E., Crickmore, N., Van Rie, J., Lereclus, D., Baum, J., Feitelson, J., Zeigler, D.R. and Dean, D.H. *Bacillus thuringiensis* and its pesticidal crystal proteins. *Microbiol. Mol. Biol. Rev.* 1998: **62**: 775-806.

[5] Knowles, B.H. and Ellar, D.J. Colloid-osmotic lysis is a general feature of the mechanism of action of *Bacillus thuringiensis* δ-endotoxins with different insect specificity. *Biochem. Biophys. Acta.* 1987; **924**: 509-518.

[6] Knowles, B.H. Mechanism of action of *Bacillus thuringiensis* insecticidal δ-endotoxins. *Adv. Insect Physiol.* 1994; **24**: 275-308.

[7] Grochulski, P., Masson, L., Borisova, S., Pusztai-Carey, M., Schwartz, J.L., Brousseau R. and Cygler, M. *Bacillus thuringiensis* CryIA(a) insecticidal toxin: crystal structure and channel formation. *J. Mol. Biol.* 1995; **254**: 447-464.

[8] Li, J., Carroll, J. and Ellar, D.J. Crystal structure of insecticidal delta-endotoxin *from Bacillus thuringiensis* at 2.5 Å resolution. *Nature* 1991; **353**: 815-821.

[9] Walters, F.S., Slatin, S.L., Kulesza, C.A. and English, L.H. Ion channel activity of N-terminal fragments from CryIA(c) delta-endotoxin. *Biochem. Biophys. Res. Commun.*. 1993; **196**: 921-926.

[10] Von Tersch, M.A., Slatin, S.L., Kulesza, C.A. and English, L.H. Membrane-permeabilizing activities of *Bacillus thuringiensis* coleopteran-active toxin CryIIIB2 and CryIIIB2 domain I peptide. *Appl. Environ. Microbiol.* 1994; **60**: 3711-3717.

[11] Gazit, E., La Rocca, P., Sansom, M.S.P. and Shai, Y. The structure and organization within the membrane of the helices composing the pore-forming domain of *Bacillus thuringiensis* delta-endotoxin are consistent with an "umbrella-like" structure of the pore. *Proc. Natl. Acad. Sci. USA* 1998; **95**: 12289-12294.

[12]. Guereca, L. and Bravo, A. The oligomeric state of *Bacillus thuringiensis* Cry toxins in solution. *Biochem. Biophys. Acta.* 1999; **1429**: 342-350.

[13] Schwartz, J.L., Juteau, M., Grochulski, P., Cygler, M., Prefontaine, G., Brousseau, R. and Masson, L. Restriction of intramolecular movements within the Cry1Aa toxin molecule of *Bacillus thuringiensis* through disulfide bond engineering. *FEBS Lett.* 1997; **410**: 397-402.

[14] Kumar, A.S. and Aronson, A.I. Analysis of mutations in the pore-forming region essential for insecticidal activity of a *Bacillus thuringiensis* delta-endotoxin. *J. Bacteriol.* 1999; **181**: 6103-6107.

[15] Masson, L., Tabashnik, B.E., Liu, Y.B., Brousseau, R. and Schwartz, J.L. Helix 4 of the *Bacillus thuringiensis* Cry1Aa toxin lines the lumen of the ion channel. *J. Biol. Chem.* 1999; **274**: 31996-32000.

[16] Gerber, D. and Shai, Y. Insertion and organization within membranes of the delta-endotoxin pore-forming domain, helix 4-loop-helix 5, and inhibition of its activity by a mutant helix 4 peptide. *J. Biol. Chem.* 2000 (in press)

[17] Uawithya, P., Tuntitippawan, T., Katzenmeier, G., Panyim, S. and Angsuthanasombat, C. Effects on larvicidal activity of single proline substitutions in α3 or α4 of the *Bacillus thuringiensis* Cry4B toxin. *Biochem. Mol. Biol. Inter.* 1998; **44**: 825-832.

[18] Sramala, I., Uawithya, P., Chanama, U., Leetachewa, S., Krittanai, C., Katzenmeier, G., Panyim, S. and Angsuthanasombat, C. Single proline substitutions of selected helices of the *Bacillus thuringiensis* Cry4B toxin affect inclusion solubility and larvicidal activity. *J. Biochem. Mol. Biol. Biophys.* 2000; **4**: 187-193.

[19] Angsuthanasombat, C., Chungjatupornchai, W., Kertbundit, S., Luxananil, P., Settasatian, C., Wilairat, P. and Panyim, S. Cloning and expression of 130-kd mosquito-larvicidal delta-endotoxin gene of *Bacillus thuringiensis* var. *israelensis* in *Escherichia coli*. *Mol. Gen. Genet.* 1987; **208**: 384-389.

[20] Angsuthanasombat, C., Crickmore, N. and Ellar, D.J. Effects on toxicity of eliminating a cleavage site in a predicted interhelical loop in the *Bacillus thuringiensis* CryIVB δ-endotoxins. *FEMS Microbiol. Lett.* 1993; **111**: 255-262.

[21] Uawithya, P., Krittanai, C., Katzenmeier, G., Leetachewa, S., Panyim, S. and Angsuthanasombat, C. 3D models for *Bacillus thuringiensis* Cry4A and Cry4B insecticidal proteins based on homology modelling. Abstract 32nd Meeting, Society for Invertebrate Pathology, Irvine, USA. 1999; p.75.

Regular Paper in Journal Biochemistry
Field: Biochemistry (I)
Topic: Biochemistry General

Expression and Biochemical Characterisation of the *Bacillus thuringiensis* Cry4B α1-α5 Pore-Forming Fragment

Theeraporn Puntheeranurak, Somphob Leetacheewa, Gerd Katzenmeier, Chartchai Krittanai, Sakol Panyim and Chanan Angsuthanasombat*

Laboratory of Molecular Biophysics, Institute of Molecular Biology and Genetics, Mahidol University, Salaya Campus, Nakornpathom 73170, Thailand

* To whom correspondence should be addressed.

Institute of Molecular Biology and Genetics, Mahidol University, Salaya Campus, Nakornpathom, Thailand 73170

Tel: (662)-441-9003 ext. 1278; Fax: (662)-441-9906; stcas@mahidol.ac.th

SUMMARY

Tryptic activation of the 130-kDa *Bacillus thuringiensis* Cry4B δ-endotoxin produced protease-resistant products of ca. 47 kDa and ca. 21 kDa. The 21-kDa fragment was identified to be the N-terminal five-helix bundle (α1-α5) which is a potential candidate for membrane insertion and pore formation. In this study, we have constructed the recombinant clone over-expressing this putative pore-forming (PPF) fragment as inclusion bodies in *Escherichia coli*. The partially purified inclusions were composed of a 23-kDa protein which cross-reacted with Cry4B antibodies and whose N-terminus was identical to that of the 130-kDa protein. Dissimilar to protoxin inclusions, the PPF inclusions were only soluble when the carbonate buffer, pH 9.0 was supplemented with 6 M urea. After renaturation *via* stepwise dialysis, the refolded PPF protein appeared to exist as an oligomer and was structurally stable upon trypsin treatment. Unlike the 130-kDa protoxin, the refolded protein was able to release entrapped glucose from liposomes and showed comparable activity to the full length activated toxin, although it lacks larvicidal activity. These results therefore support the notion that the PPF fragment consisting of α1-α5 of the activated Cry4B toxin is involved in membrane pore-formation.

Key words: *Bacillus thuringiensis*, δ-endotoxins, Liposomes, Pore formation, Refolding

INTRODUCTION

The different δ-endotoxins that are produced as cytoplasmic inclusions during sporulation by *Bacillus thuringiensis* (*Bt*) are variously active against the larvae of major insect agricultural pests and disease vectors (1,2). These parasporal crystalline inclusions are composed of one or more polypeptides of varying molecular mass that have been classified as Cry and/or Cyt δ-endotoxins according to the similarity of their deduced amino acid sequences (3,4). For instance, the 130-kDa mosquito-larvicidal protein from *Bt* subsp. *israelensis* is identified as the Cry4B toxin (2,3).

The general mechanism of gut epithelial cell disruption by the different *Bt* δ-endotoxins is thought to be the formation of lytic pores in the susceptible insect membrane (5). Upon ingestion, the inclusions are solubilised and the protoxins activated at the alkaline pH by proteases of the larval midgut. The activated toxins then bind to insect specific receptors and insert into the cell membrane to form leakage pores that result in cell death by colloid osmotic lysis (see 6 for reviews). However, an entire molecular characterisation of the pore-forming process mediated by these insecticidal proteins has not yet been obtained.

To date, two tertiary structures of different Cry toxins, Cry1Aa and Cry3A, have been resolved by X-ray crystallography (7,8). Both structures display a possible apparatus for pore formation in the form of a bundle of long amphipathic and hydrophobic helices in the N-terminal seven-helix domain (α1-α7), which could penetrate the membrane to form a transmembrane pore. The possibility that this helical structure is essential for pore formation is supported by the feature that it is conserved throughout the Cry toxin family (3,8). This is also supported by analogies with the pore-forming domain structure of two other well-characterised bacterial toxins, colicin A comprising a bundle of ten helices and diphtheria toxin consisting of a nine-helix bundle (9). Two studies with truncated proteins corresponding to the seven-helix bundle of Cry1Ac and Cry3B2 have demonstrated pore-forming activity in planar lipid bilayers (10,11). In addition, a number of studies *via* synthetic peptides or site-directed mutagenesis have provided evidence to support that α4 and α5 of several Cry toxins are involved in membrane penetration and pore formation (12-17).

Recently, we have demonstrated that α4 and α5 of the Cry4B toxin are important determinants of mosquito-larvicidal activity, likely to be involved in pore formation rather than in receptor binding (18,19). More recently, elimination of one charged residue (Arg-158) in α4 of Cry4B was found to considerably affect the toxicity (20). We also found that in addition to removal of the C-terminal half of the 130-kDa Cry4B protoxin, the activated molecule had undergone proteolytic activation producing two main sets of cleavage products at ca. 47 kDa and ca. 21 kDa (21). Aligning these positions with the Cry3A crystal structure (8) suggested that one cleavage occurred in a region before the start of the N-terminal helical bundle and the other one occurred in a predicted loop joining helices 5 and 6 in the bundle (22). This putative N-terminal five-helix bundle (α1-α5) was isolated as a protease-resistant fragment of ca. 21 kDa under denaturing conditions (22). At present, the role of this α1-α5 fragment in the Cry4B mechanism of toxicity is still not clearly understood. In this report, a recombinant clone that highly expresses this putative pore-forming (PPF) fragment has been successfully constructed. Subsequent investigation revealed that the refolded PPF protein was able to induce liposome permeability, suggesting that the α1-α5 fragment is an essential component for pore-forming activity of the Cry4B toxin.

MATERIAL AND METHODS

Construction of the Plasmid Expressing the PPF Protein

A gene segment encoding the PPF region (Met-1 to Leu-209; see Fig. 1) of the Cry4B toxin was generated by polymerase chain reaction (PCR) using the plasmid template pMU388 containing the full-length 130-kDa Cry4B toxin gene (23). Oligonucleotide primers (*universal primer*-f: 5'-TTGTGAGCGGATAACAATTTC-3'; *H5PPF*-r: 5'-GTGTACTGCA CCATGG**TTTATTA**TAGTTGGTCACCAGA-3') were purchased from Genset Inc. (Singapore). The introduced *Nco*I site is underlined and two stop codons are shown as boldface. The PCR fragment with end-repaired *BamH*I-5' and *Nco*I-3' termini was directionally cloned into end-repaired *EcoR*I and *Nco*I sites of the expression vector pMEx8 containing the *tac* promoter (24), giving the recombinant plasmid pM4BH1-5. The PPF-coding sequence was verified by DNA sequencing using an ABI prism 377 sequencer.

Expression and Preparation of the PPF Protein

The PPF protein was over-expressed in *E. coli* strain JM109 by addition of isopropyl-β-D-thiogalactopyranoside (IPTG, 0.1 mM) to mid-exponential phase cultures, and partially purified as described earlier (18). Protein concentrations were determined using a Bio-Rad protein quantitation kit. The protein inclusions (1 $mg.ml^{-1}$) were solubilised at 37 °C for 1 hr in 50 mM Na_2CO_3 buffer, pH 9.0 supplemented with 6 M urea, and any insoluble protein was removed by centrifugation in a bench minifuge at 16,000×g for 15 min. The proteins were refolded by stepwise dialysis against 300 volumes of carbonate buffers with decreasing urea concentrations of 3 M, 1.5 M, 0.75 M, 0.5 M, 0.25 M and 0.1 M at 25°C for 2-3 hrs each, and finally dialysed twice against 300 volumes of carbonate buffer.

Proteolytic stability of the refolded PPF protein was analysed by digestion with 1:50 (w/w) trypsin (L-1-tosylamide-2-phenylethyl chloromethyl ketone treated, Sigma): protein at 37 °C for 1 hr, and the samples were analysed by SDS 15% (w/v) PAGE. Immunoblotting was performed with polyclonal rabbit antibodies against the full length activated Cry4B toxin. Immunocomplexes were detected with an anti-rabbit antibody-alkaline phosphatase conjugate (Sigma). An ABI 492 automated sequencer was used to determine N-terminal sequences of the electroblotted proteins on a polyvinylidene difluoride (PVDF) membrane (Problott, Applied Biosystems).

Liposome Entrapped Glucose Release Assays

Liposomes with trapped glucose were prepared by a modified method of Kinsky (25). A lipid mixture (Sigma) of 12.5 μmole phosphatidylcholine (PC), 3.6 μmole dicetyl phosphate and 1.8 μmole cholesterol in 3 ml chloroform/methanol (2:1, v/v) was placed in a round bottomed flask and the solvent was removed under vacuum at 37°C. The resulting lipid film was resuspended in 0.5 ml of 300 mM glucose/10 mM HEPES, pH 8.0. Small unilamellar vesicles (SUVs) were prepared by squeezing the suspension through the extruder membrane (0.1 μm in diameter, Avanti Polar Lipid) for a minimum of 11 passes. Unentrapped glucose was removed from the SUV suspension by gel filtration on a PD-10 column (Sephadex G-25, Pharmacia) equilibrated 150 mM KCl/ 10 mM HEPES, pH 8.0. An aliquot of washed liposomes (100 nmole PC) was placed in a 1 ml disposable polymethyl methacrylate cuvette (Brand) containing 1 unit of hexokinase (Sigma), 1 unit of glucose-6-phosphate dehydrogenase (Sigma), 1 mM ATP, 0.5 mM NADP, 2 mM Mg $(OAc)_2$ in 150 mM KCl/ 10 mM HEPES, pH 8.0. Glucose release, detected as an increase in absorbance of NADPH at 340 nm, was monitored at 25 °C on an HP 8453 spectrophotometer (Hewlett Packard). The relative glucose-release activities are indicated as a fraction of maximum release which is defined as the amount released by 0.1% Triton X-100.

Mosquito-Larvicidal Activity Assays

Bioassays were performed as previously described using 2-day old *Aedes aegypti* larvae (19). In the assays, 1 ml of *E. coli* suspension (ca. 10^8 cells) was added to a 48-well microtitre plate (11.3 mm well diameter), with 10 larvae per well and a total of 100 larvae for each type of *E. coli* samples. *E. coli* cells containing the recombinant plasmid pMU388 were used as a positive control. Mortality was recorded after incubation for 24 hrs at room temperature (25-30 °C).

RESULTS AND DISCUSSION

In preliminary experiments, the results of size-exclusion FPLC analysis under non-denaturing conditions (carbonate buffer, pH 9.0) indicated that the 21-kDa N-terminal helix bundle (α1-α5) of the Cry4B toxin remains non-covalently associated with the C-terminal portion (ca. 47 kDa) of the activated toxin after proteolytic activation with trypsin (Angsuthanasombat, C., unpublished data). Attempts made to isolate this α1-α5 fragment by FPLC under denaturing conditions (8 M urea, carbonate buffer, pH 9.0) were unsuccessful. In this study, cloning of the PPF fragment in *E. coli* and over-expression of the protein allowed the isolation and biochemical characterisation of this PPF protein.

Upon induction with IPTG, *E. coli* cells harbouring the plasmid clone (pM4BH1-5) expressed the PPF protein at high levels in the form of sedimentable inclusion bodies with a yield of approximately 15 mg per liter of culture. Analysis of the inclusion preparation by SDS-PAGE revealed a major band at 23 kDa (see Fig. 2A) which specifically cross-reacted in Western blots probed with antibodies raised against the activated Cry4B toxin (Fig. 2B). The N-terminal sequence of the 23-kDa protein obtained by automated Edman degradation was found to be identical to the N-terminus of the 130-kDa protoxin (MNSGY). Since the predicted molecular mass of the polypeptide encoded in the cloned PPF fragment is 23.587 kDa, these results provide evidence that the 23-kDa product we have obtained from over-expressing *E. coli* corresponds to the N-terminal α1-α5 segment of the Cry4B toxin.

Unlike the inclusions of the full length protoxin (1 $mg.ml^{-1}$) which are soluble (up to 80%) in carbonate buffer, pH 9.0 (18), the PPF inclusions (1 $mg.ml^{-1}$) were readily soluble only in the presence of 6 M urea, giving at least 60% solubility. The PPF protein was refolded by stepwise dialysis against buffers with decreasing urea concentrations and finally

the protein was obtained in urea-free carbonate buffer, pH 9.0 at a concentration of 0.5 $mg.ml^{-1}$. The refolded PPF preparation (Fig. 3, lane 3) was subjected to size-exclusion FPLC using a Sephacryl S-100 column (Pharmacia) with carbonate buffer, pH 9.0 as eluent at a flow rate of 0.5 $ml.min^{-1}$. Elution of the protein was monitored at 280 nm and the 23-kDa PPF protein was eluted in the void volume of the column (data not shown). This suggested that a high molecular mass (> 300 kDa) oligomer or aggregate was present rather than the monomeric form of the refolded PPF protein. Notwithstanding this observation, this aggregate could represent a stable and functional oligomerisation state of the PPF fragment with the ability to intercalate into lipid membranes to form a pore. Interestingly, treatment of the refolded 23-kDa PPF protein with trypsin resulted in a 21-kDa protein fragment detectable by SDS-PAGE (see Fig. 3, lane 4) which specifically cross-reacted with Cry4B toxin antibodies (data not shown). We conclude that this 21-kDa PPF protein is structurally resistant to further proteolysis and that the refolded 23-kDa PPF protein likely exists in its native folded conformation. Proteins which are extensively resistant to proteolysis have been shown to maintain a significant portion of native-like conformation (26).

No significant activity was observed in bioassays against *Aedes aegypti* larvae using *E. coli* cells expressing the PPF protein. Lack of toxicity is most likely due to the absence of a three-β-sheet domain (8) which is required for binding of the activated toxin to larval midgut epithelial cells *via* specific receptors. It is still an open question whether after proteolytic activation *in vivo*, the bundle of five helices remains associated with the 47-kDa fragment containing the receptor-binding domain in the pore-forming process. In other studies with the Cry4A cleavage products genetically fused with glutathione S-transferase (GST), significant larvicidal activity was observed only when both of the fusion proteins, GST-20-kDa (α1-α5) and GST-45-kDa containing the receptor-binding domain, were co-ingested by the larvae (27).

The membrane lytic capability of the refolded PPF protein was assayed for its ability to release glucose from receptor-free phospholipid vesicles. Under the conditions used in this assay, the refolded PPF fragment was able to induce release of entrapped glucose from liposomes and the release activity depended on the concentration of the protein used (see Fig. 4). Approximately 47% of maximum release (when compared to Triton X-100 as a positive control) was observed within 10 min after addition of the protein (15 $\mu g.ml^{-1}$ or ca. 0.6 mM). These results are consistent with former findings that the N-terminal α-helical bundles of the Cry1Ac and Cry3B2 toxins were able to mediate the release of ^{86}Rb cation from phospholipid vesicles and form cation selective channels in planar lipid bilayers (10,11). At the equivalent molar concentration to that of the PPF protein, the full length activated Cry4B toxin (45 $\mu g.ml^{-1}$) exhibited similar activity in the glucose release assays whereas the 130-kDa protoxin (90 $\mu g.ml^{-1}$) and a control sample containing carbonate buffer (50 mM Na_2CO_3, pH 9), showed little glucose release (< 10%). Similarly, it was reported by other workers that the full length activated toxins of Cry1Aa (ca. 65 kDa), Cry1Ac (ca. 55 kDa) and Cry1C (ca. 67 kDa) were able to form channels in planar bilayers in the concentration range of 15-32 $\mu g.ml^{-1}$ (15,28,29). However, the stimulus for channel formation is still unclear. High toxin concentrations might be sufficient to obviate the requirement for a receptor, which might favour spontaneous membrane insertion of the toxins.

In summary, our results demonstrate that the 23-kDa α1-α5 fragment is fully capable of permeabilising the membrane liposomes *in vitro* apart from the rest of the activated Cry4B toxin, and therefore constitutes the region responsible for membrane insertion and pore formation within the Cry toxin molecules. The cloned PPF fragment will facilitate further investigations on the pore-forming mechanism of the Cry insecticidal toxins.

toxin molecule of *Bacillus thuringiensis* through disulfide bond engineering. *FEBS Lett.* **410**, 397-402.

16 Kumar, A.S., and Aronson, A.I. (1999) Analysis of mutations in the pore-forming region essential for insecticidal activity of a *Bacillus thuringiensis* delta-endotoxin. *J. Bacteriol.* **181**, 6103-6107.

17 Masson, L., Tabashnik, B.E., Liu, Y.B., Brousseau, R., and Schwartz, J.L. (1999) Helix 4 of the *Bacillus thuringiensis* Cry1Aa toxin lines the lumen of the ion channel. *J. Biol. Chem.* **274**, 31996-32000.

18 Uawithya, P., Tuntitippawan, T., Katzenmeier, G., Panyim, S., and Angsuthanasombat, C. (1998) Effects on larvicidal activity of single proline substitutions in α3 or α4 of the *Bacillus thuringiensis* Cry4B toxin. *Biochem. Mol. Biol. Inter.* **44,** 825-832.

19 Sramala, I., Uawithya, P., Chanama, U., Leetachewa, S., Krittanai, C., Katzenmeier, G., Panyim, S. and Angsuthanasombat, C. (2000) Single proline substitutions of selected helices of the *Bacillus thuringiensis* Cry4B toxin affect inclusion solubility and larvicidal activity. *J. Biochem. Mol. Biol. Biophys.* **4**, 187-193.

20 Sramala, I., Leetachewa, S., Krittanai, C., Katzenmeier, G., Panyim, S. and Angsuthanasombat, C. (2000) Screening charged residues in helix 4 of the *Bacillus thuringiensis* Cry4B toxin reveals one critical residue for larvicidal activity. *J. Biochem. Mol. Biol. Biophys.* (in press).

21 Angsuthanasombat, C., Crickmore, N., and Ellar, D.J. (1991) Cytotoxicity of a cloned *Bacillus thuringiensis* subsp. *israelensis* CryIVB toxin to an *Aedes aegypti* cell line. *FEMS Microbiol. Lett.* **83**, 273-276.

22 Angsuthanasombat, C., Crickmore, N., and Ellar, D.J. (1993) Effects on toxicity of eliminating a cleavage site in a predicted interhelical loop in the *Bacillus thuringiensis* CryIVB δ-endotoxins. *FEMS Microbiol. Lett.* **111**, 255-262.

23 Angsuthanasombat, C., Chungjatupornchai, W., Kertbundit, S., Luxananil, P., Settasatian, C., Wilairat, P., and Panyim, S. (1987) Cloning and expression of 130-kd mosquito-larvicidal delta-endotoxin gene of *Bacillus thuringiensis* var. *israelensis* in *Escherichia coli. Mol. Gen. Genet.* **208**, 384-389.

24 Buttcher,V., Ruhlmann, A., and Cramer, F. (1990) Improved single-stranded DNA producing expression vectors for protein manipulation in *Escherichia coli. Nucleic Acids Res.* **18**, 1075.

25 Kinsky, S.C. (1974) Preparation of liposomes and a spectrophotometric assay for the release of trapped glucose marker. *Meth. Enzymol.* **32**, 501-513.

26 Fontana, A., Polverino de Laureto, P., De Filippis, V., Scaramella, E., and Zambonin, M. (1997) Probing the partly folded states of proteins by limited proteolysis. *Folding & Design.* **2**, R17-R26.

27 Yamagiwa, M., Esaki, M., Otake, K., Inagaki, M., Komano, T., Amachi, T. and Sakai, H. (1999) Activation process of dipteran-specific insecticidal protein produced by *Bacillus thuringiensis* subsp. *israelensis. Appl. Environ. Microbiol.* **65**, 3464-3469.

28 Slatin, S.L., Abrams, C.K., and English, L. (1990) Delta-endotoxins from cation-selective channels in planar lipid bilayers. *Biochem. Biophys. Res. Commun.* **169**, 765-722.

29 Schwartz, J.L., Garneau, L., Masson, L., Brousseau, R., and Rousseau, R. (1993) Lepidopteran-specific crystal toxins from *Bacillus thuringiensis* form cation- and anion-selective channels in planar lipid bilayers.*J. Membr. Biol.* **132**, 53-62.

Fig. 1. **Tryptic processing of the 130-kDa Cry4B protoxin.** An overview of the results obtained from N-terminal sequencing of trypsin-treated products of Cry4B. The arrows indicate the known cleavage sites within the toxin. The region between Met-1 and Leu-209 represent the PPF fragment.

Fig. 2. **Expression of the PPF protein in *E. coli.*** (A): A Coomassie brilliant blue-strained SDS-15 % polyacrylamide gel showing the total crude extracts (T) of *E. coli* cells harbouring the pMEx8 vector or the pM4BH1-5 recombinant encoding the PPF protein. (B): Immunoblot analysis of (A) showing the 23-kDa PPF protein cross-reacted with Cry4B antibodies. (M) represents molecular mass standards. (S) and (P) are the supernatant and pellet fractions, respectively.

Fig. 3. **SDS-PAGE (15% gel) analysis of tryptic processing of Cry4B and the PPF protein.** M represents molecular mass standards. Lane 1 is the 130-kDa solubilised protoxin. Lane 2 is the activated toxin. Lanes 3 and 4 are refolded PPF and the refolded protein treated with trypsin (1:50 enzyme:protein, w/w), respectively.

Fig. 4. **Effect on glucose release from liposomes.** (A): Release of entrapped glucose was monitored by using NADP-linked enzyme-linked assays at 25 °C. The traces represent absorbance at 340 nm which was continously recorded for 5 min prior to adding each protein sample as indicated by an arrow. The maximum release was obtained by adding 0.1% Triton X-100 (indicated by a vertical bar) after 10 min incubation with samples; (a) 100 µl carbanate buffer, (b) 15 $\mu g.ml^{-1}$ refolded PPF, (c and d) 15 and 45 $\mu g.ml^{-1}$ activated Cry4B and (e and f) 45 and 90 $\mu g.ml^{-1}$ 130-kDa protoxin. (B): The relative release activities of each protein sample with varying concentrations that are indicated as fraction of 100% release induced by Triton X-100. Error bars represent standard error of the mean from five separate experiments. The release in the control sample incubated with carbonate buffer rarely exceeded 10% and these values have been subtracted in the figure.

Figure 1

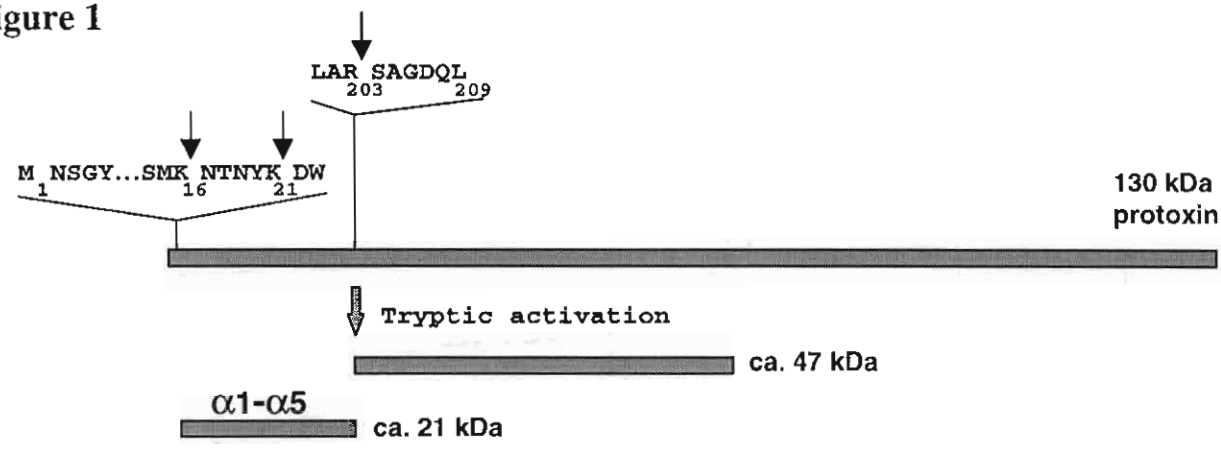

Figure 2

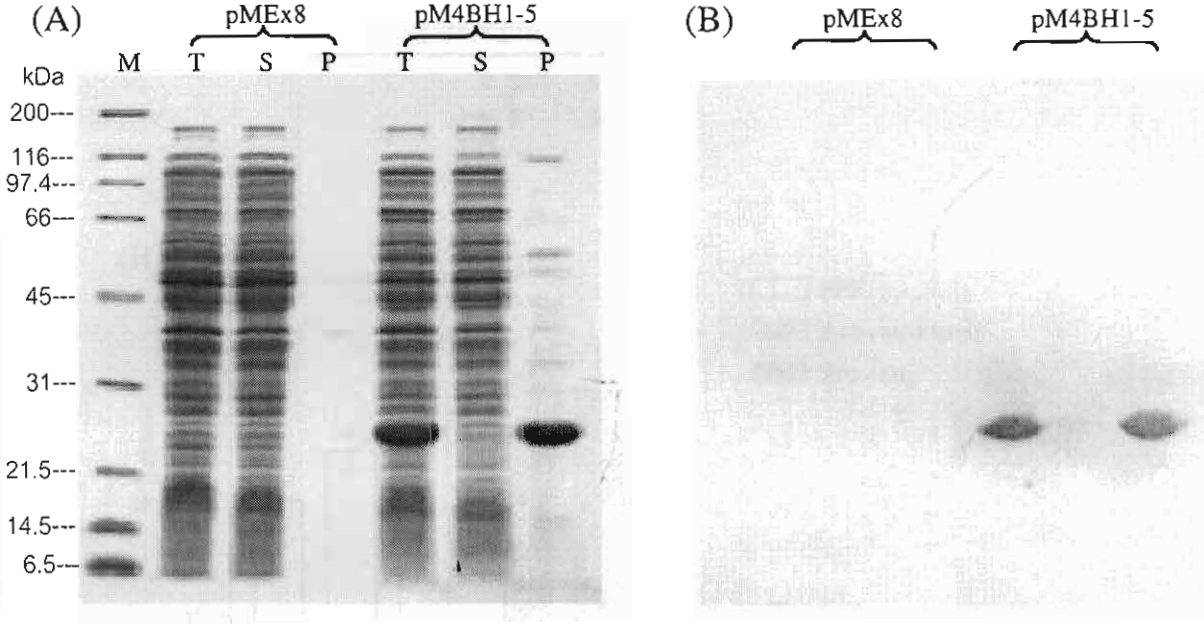

Figure 3

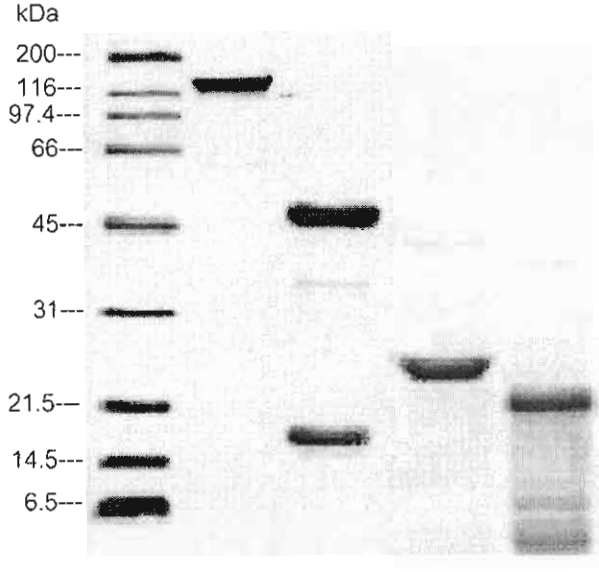

Figure 4

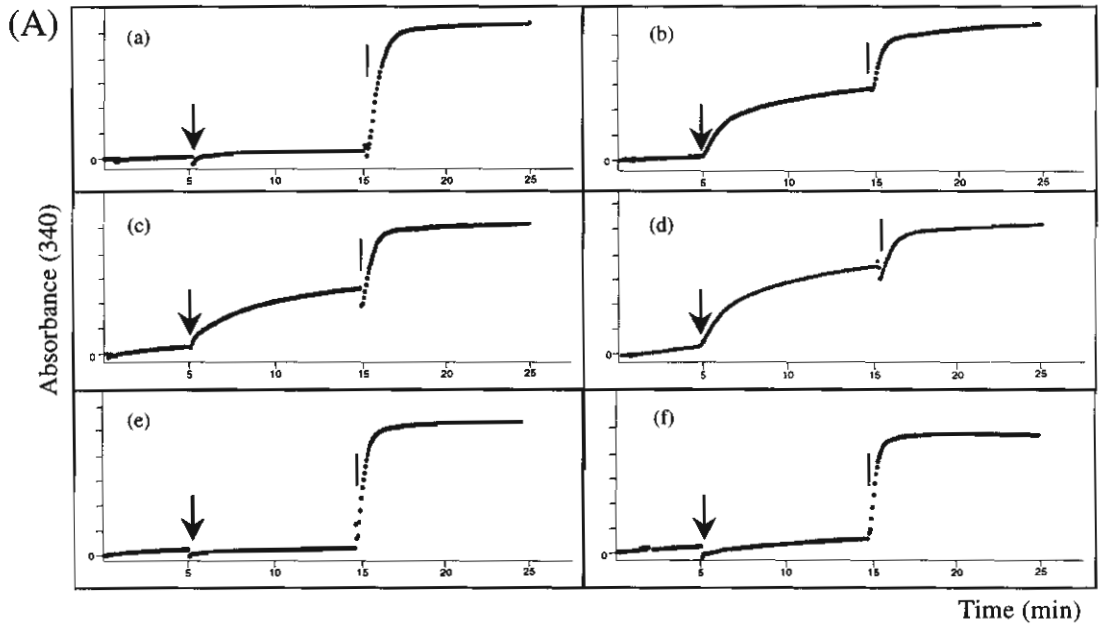
(A)
(a)
(b)
(c)
(d)
(e)
(f)
Absorbance (340)
Time (min)

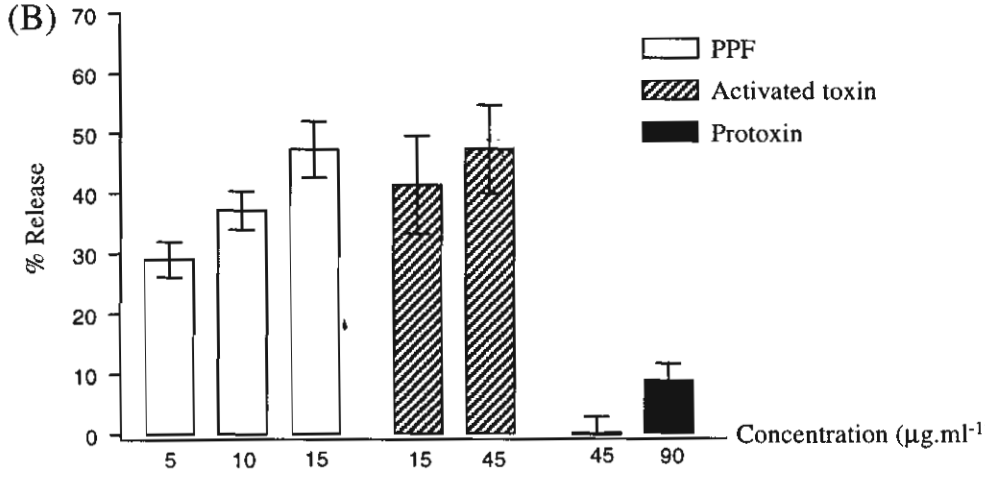
(B)
% Release
PPF
Activated toxin
Protoxin
Concentration (µg.ml-1)